



T.C.

ALTINBAS UNIVERSITY

Information Technology

MEDICAL VIDEO ENHANCEMENT

Ahmed Rashid Ibrahim ALABD

M. Sc. Thesis

Supervisor

Prof. Dr. Osman Nuri UCAN

Istanbul, 2019

MEDICAL VIDEO ENHANCEMENT

by

Ahmed Rashid Ibrahim Alabd

INFORMATION TECHNOLOGY

Submitted to the Graduate School of Science and Engineering

in partial fulfillment of the requirements for the degree of

Master of Science

ALTINBAŞ ÜNİVERSİTESİ

2019

This is to certify that we have read this thesis and that in our opinion it is fully adequate, in scope and quality, as a thesis for the degree of Master of Science.

Prof. Dr. Ziad Mohamed ABOOD

Co-Supervisor

Prof. Dr. Osman Nuri UCAN

Supervisor

Examining Committee Members (first name belongs to the chairperson of the jury and the second name belongs to supervisor)

Prof. Dr. Osman Nuri UCAN	School of Engineering and Natural Sciences, Altinbas University	_____
Prof. Dr. Oguz BAYAT	School of Engineering and Natural Sciences, Altinbas University	_____
Prof. Dr. Hasan H. BALIK	Air Force Academy, National Defense University	_____

I certify that this thesis satisfies all the requirements as a thesis for the degree of Master of Science.

Asst. Prof. Oguz ATA

Head of Department

Prof. Dr. Oguz BAYAT

Director

Approval Date of Graduate School of
Science and Engineering: ____/____/____

I hereby declare that all information in this document has been obtained and presented in accordance with academic rules and ethical conduct. I also declare that, as required by these rules and conduct, I have fully cited and referenced all material and results that are not original to this work.



Ahmed Rashid Ibrahim

ACKNOWLEDGEMENTS

First of all, thanks to Almighty Allah who has given us courage wisdom to complete this work and patience to face all difficulties.

Foremost, I would like to express my sincere gratitude to my co-advisor Prof. Dr. Ziad Mohamed ABOOD and my advisor Prof. Dr. Osman Nuri UCAN for the continuous support of my study and research, for his patience, motivation, enthusiasm and immense knowledge. This work would not have been possible without his guidance, support and encouragement. Under his guidance, I successfully overcame many difficulties and learned a lot. His invaluable guidance and support at every stage have led to the successful conclusion of the study.

Finally, I want to convey my special thanks to my mother, my father for her love and continuous encouragement for me, my brother, and friends their call and moral support have been invaluable at every stage of my life. Thank you all for standing by me at all times.

ÖZET

MEDİKAL VIDEO GELİŞTİRME

AHMED RASHID IBRAHIM ALABD

Yüksek Lisans, Bilişim Teknolojileri, Altınbaş Üniversitesi,

Danışman: Prof. Dr. Osman Ucan

İkincil Danışman: Prof. Dr. Ziad Mohamed Abood

Tarih: 06/2019

Sayfa Sayısı: 88

Medikal Video ve renkli ve siyah-beyaz Medikal görüntüler için video geliştirme algoritmasının kullanılması, matlab Programlarını kullanarak. Video geliştirme, video araştırmasında en önemli ve zorlu bileşenlerden biridir. Video geliştirmenin amacı, videonun görsel görünümünü geliştirmek veya analiz, tespit, bölümlendirme, tanıma, gözetleme, trafik, ceza adalet sistemleri gibi gelecekteki otomatik video işleme için “daha iyi” bir dönüşüm sunumu sağlamaktır. Mevcut video geliştirme teknikleri iki kategoride sınıflandırılabilir: Kendini geliştirme ve İçerik esaslı füzyon geliştirme. Daha spesifik olarak, video geliştirme temsili tekniklerini temel alan işleme yöntemlerini sınıflandırıyoruz.

Anahtar Kelimeler: kontrast filtresi, Tıbbi video, Retinex teorisi, Video geliştirme, Video çerçeve.

ABSTRACT

MEDICAL VIDEO ENHANCEMENT

AHMED RASHID IBRAHIM ALABD

M. Sc. Information Technology, Altınbaş University,

M. Sc. Thesis

Supervisor: Prof. Dr. Osman Nuri Ucan

Co-Supervisor: Prof. Dr. Ziad Mohamed Abood

Date: 06/2019

Pages: 88

Using video enhancement algorithm for Medical Video and with color and black & white Medical images, by using matlab Programs. Video enhancement is one of the most important and default components in video research. The aim of video enhancement is to improve the visual appearance of the video, or to provide a better transform representation for future automated video processing, such as analysis, detection, segmentation, recognition, surveillance, tract, criminal justice systems. The existing techniques of video enhancement can be classified into two categories: Self-enhancement and Context based fusion enhancement. More specifically, we categorize processing methods based representative techniques of video enhancement.

Keywords: Contrast Filter, Medical Video, Retinex Theory, Video Enhancement, Video Frame.

TABLE OF CONTENTS

	<u>Pages</u>
ABSTRACT.....	vii
LIST OF TABLES.....	xi
LIST OF FIGURES.....	xii
1. GENERAL INTRODUCTION.....	1
1.1 TYPES OF DIGITAL IMAGES.....	2
1.1.1 Binary Images.....	2
1.1.2 Gray Scal Images.....	2
1.1.3 Color Images.....	3
1.1.4 Multi-Spectral Images.....	3
1.2 DIGITAL IMAGE PROCESSING STAGES.....	4
1.3 LITERATURER REVIEW.....	5
1.4 OBJETIVES OF THE STUDY.....	6
1.5 THESIS LAYOUT.....	6
2. THEORITICAL PART.....	7
2.1 IMAGE PROCESSING.....	7
2.2 GOALS OF MEDICAL IMAGE ANALYSIS TECHNIQUES.....	7
2.2.1 Medical Image Processing.....	7
2.2.2 The Quality of the Medical Image.....	8
2.3 INDICATION FOR CARDIAC CATHETERIZATION.....	10
2.3.1 Design Of The Catheterization Protocol.....	11
2.3.2 Image Display and Processing.....	11
2.3.3 Flat-panel and Xray	12
2.3.4 Catheter.....	13
2.3.5 Prepare for Catherization.....	13

2.3.6 How it works Catheter.....	13
2.3.7 Risks of Heart Catheterization.....	14
2.4 IMAGE ENHANCEMENT.....	14
2.4.1 Approaches of Image Enhancement.....	15
2.5 FILTERS.....	15
2.6 VIDEO ENHANCEMENT.....	16
2.6.1 Pre-Processing.....	19
2.6.2 Reduction of Noise.....	19
2.6.3 Contrast Enhancement Methodology.....	20
2.6.4 Self-Enhancement of Poor Quality Video.....	20
2.6.5 HDR-Based Enhancement of Videos.....	20
2.7 ABOUT THE NEXT CHAPTER.....	23
2.8 VIDEO FRAME BEFORE ENHANCEMENT.....	23
2.8.1 Representativeness Learning	24
2.9 EXTRACT MOVIE FRAME.....	25
2.9.1 From Video to Image.....	26
2.10 THE FIRST METHOD (RETINEX).....	27
2.10.1 Retinex Theory.....	27
2.10.2 Image of Classification.....	29
2.10.3 MultiScale Retinex Algorithm.....	31
2.10.4 MSR with Color Restoration (MSRCR).....	32
2.10.5 Retinex Operators.....	34
2.11 WAVELET TRANSFORM (WT).....	35
2.11.1 Applications of Wavelet Transform.....	35
2.11.2 Properties of Wavelet transform.....	36

2.11.3	Edge with Wavelet (Strengthen the edge with wavelet.....)	37
2.11.4	Mathematical Expression for Wavelet Transform.....	38
2.11.5	Types of Wavelet Transform.....	38
2.12	NOISE OF IMAGE.....	40
2.12.1	Noise Types.....	40
2.13	CONTRAST AND BRIGHTNESS (CB).....	41
2.13.1	Brightness.....	41
2.13.2	Contrast.....	42
2.14	OBJECTIVE QUALITY METRICS USED IN STUDY.....	42
3.	PRACTICAL PART.....	47
3.1	INTRODUCTION.....	47
3.2	DATABASE STUDY (VIDEOS).....	47
3.3	BLOCK DIAGRAM OF STUDY.....	50
3.4	THE ALGORITHM OF STUDY.....	51
3.5	VIDEO CUTTING AND SPLITE.....	54
3.6	OPTIMIZE IMAGE USING WAVEGUIDE TECHNOLOGY.....	54
4.	FINDINGS AND CONCLUSIONS.....	57
4.1	INTRODUCTION.....	57
4.2	VIDEO ENHANCEMENT	57
4.3	DISCUSSION AND CONCLUSIONS.....	70
4.4	FUTURE WORKS.....	70
	REFERENCES.....	71
	APPENDIX A.....	78
	APPENDIX B.....	83

LIST OF TABLES

	<u>Pages</u>
Table 3.1: The Study Database (Videos) That Represent Medical Videos.....	47
Table 3.2: Videos details at table	48
Table 4.1 The quality measurements of the image (Angina pectrios) after the application of wavelet (Haar)	57
Table 4.2: The quality measurements of the image (Angina pectoris) after the application Retinex method.....	62
Table 4.3: The quality measurements of the video background enhancement	66

LIST OF FIGURES

	<u>Pages</u>
Figure 1.1: Example of binary image.....	2
Figure 1.2: Example grayscale image	3
Figure 1.3: Example color image.....	3
Figure 1.4: Example Multi-Spectral Images.....	4
Figure 2.1: Digital image.....	7
Figure 2.2: Computer aided diagnosis	7
Figure 2.3: Modulation Transfer Function	8
Figure 2.4: MTF Modulation Transfer Function	9
Figure 2.5: Zoom differences between image intensifiers and flat-panel detectors	12
Figure 2.6: CATHER	13
Figure 2.7: Enhanced video diagram	19
Figure 2. 8: (a) Original nighttime video frame, (b) Improved night-time video uses tone mapping approach	21
Figure 2.9: Molecular conversion representation (frequency division to time)	36
Figure 2. 10: Fourier representation (frequency-to-time division)	37
Figure 3.1: The General Diagram of present study.....	50
Figure 3.2: Extract Frames from Video	51
Figure 3.3: Wavelet denoising method	52
Figure 3.4: Retinex method	53
Figure 3.5: Video cutting and split into frames	54
Figure 3.6: Reading the image in the Wavelet transform.....	55
Figure 3.7: Selection of the wave and level conversion class	55

Figure 3.8: The approximate image resulting from the process of analysis and dissolution using waveguide.....56



1. GENERAL INTRODUCTION

The dramatic development of information technology has led to increased use of digital images and increased need for the development of many digital processing techniques. For the purpose of analyzing and extracting important information from images for use in various application fields (industrial, military and agricultural). The proliferation of digital image processing methodologies is the result of extensive research and studies conducted in the last three decades of the last century. Information exchange systems is in line with the development of computer systems, increasing the capacity of the treasury and the speed of processing of digital data, facilitating the circulation of information and processing, whether audio, text or visual. The image is one of the most important and most important diagnostic information.

The Picture is a description of the visual sensitivity change of the surface to be visually recorded, and the standard images resulting from the change of light intensity at the 2-D level usually produced in the sensor of the reflection signals (Reflection or Permeability), and the collection and recording of images and objects by chemical sensors film segments or electronic sensors such as (charge coupled devise) CCD camera The development of technology in recent decades led to the development and development of multi-image recording devices such as thermal cameras, radars, X-ray and ultrasound The image cannot usually be obtained from its source with perfect accuracy for many reasons, including the limitations of the visual system and its lack of idealism, due to unavoidable defects in imaging systems in addition to the external influences from atmospheric conditions, body motions or imaging. Throughout the image capture process, these defects all degrade image quality (IQ) resulting from imaging systems, so these distortions must be addressed to obtain good images that can be analyzed and used. It has developed and developed many deformation techniques, and many filtering techniques have been used to eliminate the noise associated with digital images and reduce their impact. However, most of the processing processes are not completely flawless, but sometimes improve locations and distort other locations [1].

1.1 TYPES OF DIGITAL IMAGES

Digital Images are, in general, categorized to four main types [2], [3]:

1.1.1 Binary Images

One of the simplest digital image types are the binary images, they could be either white (1) or black (0), that is only take a single binary number for every element (Pixel) of image. Examples of this type are written. Fig Example of binary image (1.1) is shows a binary image example [2].

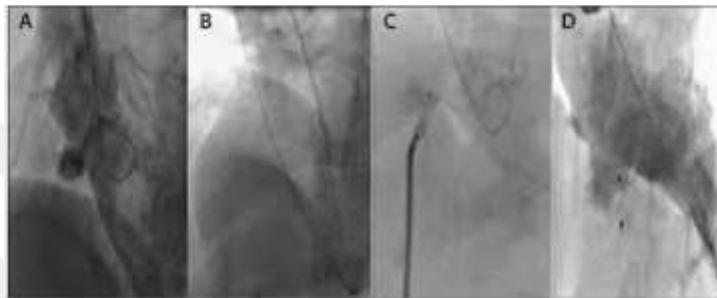


Figure 1.1: Example of binary image

1.1.2 Grayscale Images

Are monochrome images that contain only luminance levels and contain no gradients, and the value of every one of the elements in the image determines the grayscale (0-255), and each of its elements represents 8 bits/ pixel [2]. In certain applications such as Medical imaging is often represented as 12 bit / pixel or 16 bit/pixel. This increase in intensity levels is useful only when a small area of the image has a high intensity. In this case, details that may be difficult to see without this increase levels of intensity. Figure 1.2 is shows grayscale image example grayscale image.

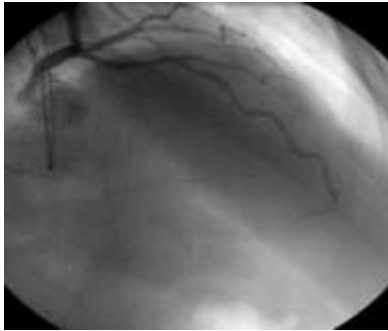


Figure 1.2: Example of grayscale image

1.1.3 Color Images

These images are represented in a three bands monochromatic data format, each of which returns to the luminance in each of the red (R), green (G), and blue (B) colours using 8 bits per element. For each color pack bands, the color image is represented by (24bits). Total of the real colors in the picture is about 16 million equivalent $(2^8)^3$. Figure 1.3 is shown color image.



Figure 1.3: Example colour image

1.1.4 Multi-Spectral Images

Multi-spectral images contain information beyond the limits of visual perception, containing data collected in several packages from infrared, ultraviolet (UV), or x-ray (satellite) images. These images are collected in several packages ranging from spectral package, one to three of these packets fall within the Visible Spectrum range, while the other beams are located in invisible areas [4], [5]. Figure (1.4) is shown Multi-Spectral image.

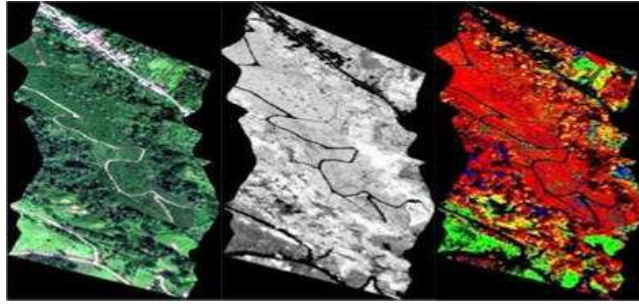


Figure 1.4: Example Multi-Spectral Images

1.2 DIGITAL IMAGE PROCESSING STAGES

One of the computer science branches is the image processing, this field is concerned with performing operations on the image with the aim of improving it on the basis of certain criteria, or extracting some data from those images. The conventional system of image processing is made up of 6 successive stages, which are ordered [6], [7]:

- Image Acquisition: using an optical sensor, for instance, laser sensor and camera.
- Primary processing such as De-noise.
- Segmentation of the image (segmentation) for separating significant information concerning the background
- Extracting features or attributes (Features Extraction).
- Classifying characteristics) and linked to the pattern and the return to identify patterns.
- Image Understanding.

(And not condition the traffic always in all stages).

1.3 LITERATURE REVIEW

1. (Lain and David, 1996) [8] Conversion of wavelets to remove noise (De-noise) of medical images and make them sharper than the original image.
2. (Sonja et.al; 2001) [9] examined a set of wavelets for application in the fixed image compression system to analyze the performance of the compressed image using wavelets, and indicated that image quality is low by compressions and disintegration using the wavelet.
3. (Damon and Sheila; 2007) [10] proposed an effective measure to measure or determine the visual accuracy of natural images referred to as Visual Signal-to-Noise Ratio (VSNR), according to the human vision characteristics close to Near-threshold and supra-threshold.
4. A new image database called TID2008: Tampere Image Database (2008) was developed by researcher (Nikolay et.al; 2009) [11] describing the assessment of the full reference to visual quality estimation measures. This database included 1700 experimental images and 25 reference photos and 17 kinds of distortion for every one of the reference images. It was concluded that the Mean Opinion Score (MOS) of the database (TID2008) may be utilized to effectively test various visual quality standards in addition to the design of new standards. Utilizing the designed image data-base, Quality standards are known.
5. Hamza et al. (2009) [12] proposed a new mechanism for the assessment of the quality of photos produced by the American College of Radiation (ACR) model using the Template Matching with Cross-Correlation method to automatically monitor the quality of mammography.
6. (Vora et.al; 2010) analyzed the compressed image quality evaluation by suggesting that the objective image quality evaluation for measuring the quality of the compressed gray image based on JPEG and JPEG-2000 had a good relation with the MOS and took less Time interval There is also a precision between the main objective measure and the self-measurement (MOS).
7. Lin Zhang et.al (2010)[13] developed a new measure of image quality assessment called the Feature Similarity Based on Riesz Transforms (RFSIM), the human vision system (HVS) realizes the image mostly based on its low-level characteristics.
8. Lin Zhang et.al (2011)[18] developed a new measure of image quality assessment called the feature Similarity (FSIM) index, which was developed according to the hypothesis that the human vision system (HVS) The image explains based on low level features.
9. (Ravi; 2012) [19] analyzed the comparison of quality standards for the treatment of medical images. The image has been applied to different proportions of blur, noise, pressure and contrast

levels, after which the image quality was measured using quality measures like (Maximum Difference-MD, MSE, PSNR, SSIM, and so on).

10. (Kanwaljot et.al; 2012) [20] used to convert wave type and dopchis waveforms to determine image quality and reduce noise level. First, the image will be decomposed through the use of Har and Dupshis transforms. Physical and non-physical threshold level is then determined for decreasing the image's noise and then via estimating and comparing PSNR from the image of each wavelet and then assigning the wavelets that give more PSNR picture.

1.4 OBJECTIVES OF THE STUDY

The current study has the aim of the enhancement of angina pectoris by enhancement the contrast of images and obtaining better image characteristics that help in better medical diagnosis. The Retinex model was used for video computing through two paths: the first is to apply the model directly to the video, and the second, to convert the video into a frame.

1.5 THESIS LAYOUT

The current study included four chapters

- Chapter one: General introduction on the importance of image processing and medical image types, the most important previous studies, the goals of the study, and finally its general structure.
- Chapter two: dealt with the theoretical aspect.
- Chapter three: contains the study samples (videos and image angina pectrois), the study algorithm, the video technique of the Retinex, the waveguide technique, and the improvement of the video used to reach the study objectives.
- Chapter four: included the results of processing video and images after the application of Retinex methods and conversion to the results of video quality measurements and images and conclusions and recommendations.

2. THE THEORETICA PART

2.1 IMAGE PROCESSING

The definition of an image is that it is a two-dimensional function $f(x, y)$, in which x and y both may be considered as the spatial (plane) coordinates, the amplitude regarding f at each one of the coordinate pairs (x, y) will be called as a gray level intensity related to an image at particular point, the values of the amplitude of f are all finite and discrete quantities. Area of digital image processing indicates the processing of images with the use of a computer. It is worth noting that the digital images are made up of a finite number of elements, every element has a specific location and value. Such elements are known as image elements, shown as in figure , Figure 2.1, picture elements, pixels and pels. “Pixel” is a word which is most commonly utilized for referring to digital image elements [14].

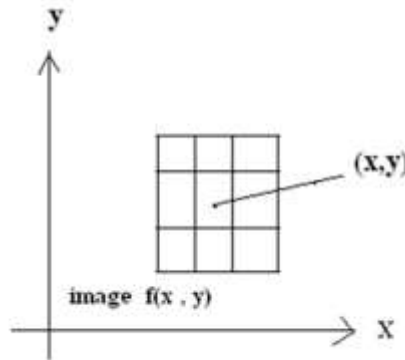


Figure 2.1: Digital image

2.2 GOALS OF MEDICAL IMAGE ANALYSIS TECHNIQUES

1- Quantification: Measuring the features on medical images, eg., radiologist obtain measurements from medical images (e.g., area or volume).

2- Computer Aided Diagnosis (CAD): given measurements shown in Figure 2.2 and features make a diagnosis. Help radiologists on their diagnosis procedure for accuracy and efficiency.

3- Evaluation and validation techniques [15].

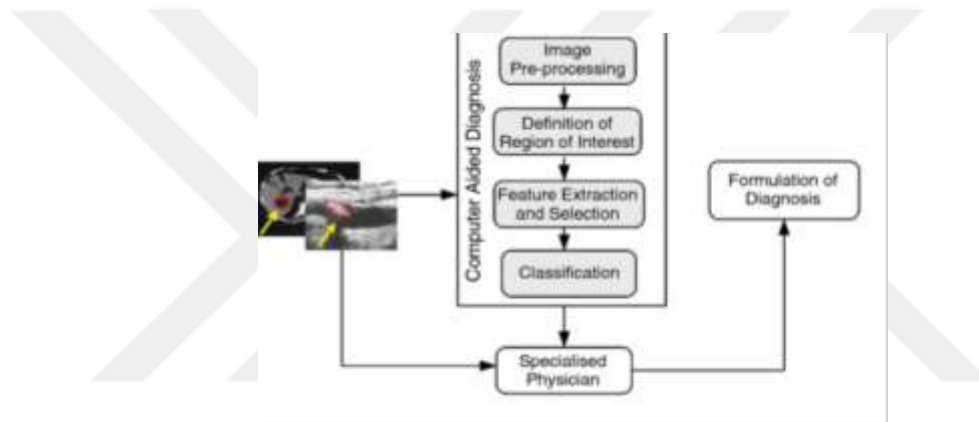


Figure 2.2: computer aided diagnosis

2.2.1 Medical Image Processing

We will explain medical image processing in the following points:-

1. Is concerned with developing problem specific methods for the enhancement of the raw medical data for selective visualization purposes and further analysis.
2. Its emphasis is focused on developing approaches for supplementing the typically qualitative and frequently subjective evaluation of medical images which is made by human experts.
3. Medical image analysis
4. Ensures quantitative, reproducible and objective information which is obtained from medical images [15].

2.2.2 The Quality of the Medical Image

The medical image quality is assessed with the precision of particular information that is searched for in an image via the observing expert. Nevertheless, objective image quality features must be determined for the sake of the evaluation of the quality of the images which is generated by a processing technique or by an imaging system.

Image sharpness, concerns mainly the ability to distinguish image detail. Image detail deterioration or blurring is mainly due to the imaging system's impulse response, the so called Point Spread Function (PSF). Image sharpness is assessed by the image spatial resolution. The latter is characterized as the capability of the imaging system in distinguishing (i.e. clearly display) two small high contrast dots close to each other. Quantitatively, the spatial resolution is defined by the minimum distance between two distinguishable high contrast points or by the magnitude of the FWHM ("Full Width at Half Maximum") or by the LSF (the number of distinguishable lines per cm) or Figure 2.3 by the MTF (Modulation Transfer Function). Figure 2.4 gives the meaning of the PSF, while it shows the distance FWHM, which is the limit of the distance that the two point sources should differ in order to be distinguishable. Another way of quantifying Image Sharpness is the MTF, which in effect is the Fourier Transform (FT) of PSF. It defines cut-off frequency f_{co} at 5% of its maximum magnitude [16].

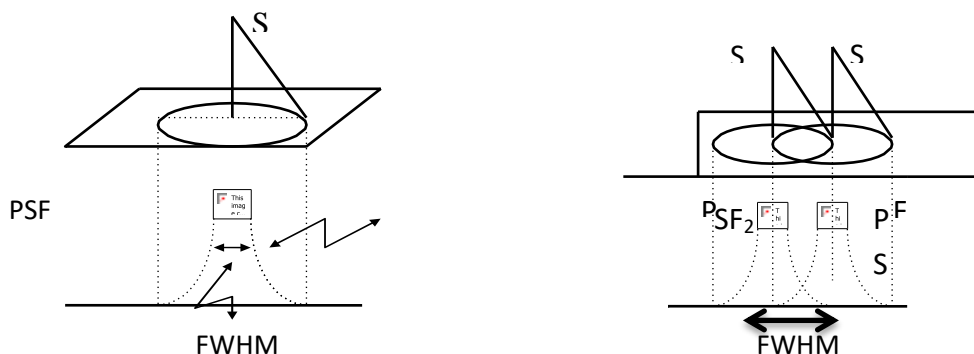


Figure 2.3: Modulation Transfer Function

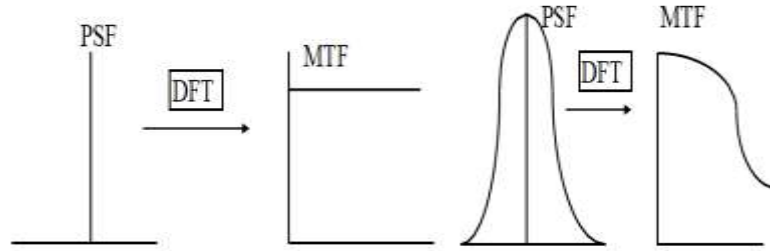


Figure 2.4: MTF Modulation Transfer Function

Image contrast concerns the ability to distinguish image detail of low contrast with its surrounding background. In other words, it is the capability of the imaging system to sense small variations in radiation intensity at its detector end and to display that intensity variation. A source of image contrast degradation is the existence of noise. For the assessment of image contrast the term contrast resolution is used and it can be characterized as the smallest distinguishable intensity difference between a small image area (of specific shape and size) and its background. Image contrast can be quantified by equation:

$$\text{contrast \%} = \frac{I_{\text{area}} - I_{\text{background}}}{I_{\text{background}}} \times 100 \quad (2.1)$$

Image noise is of statistical nature and signal dependent but, without great loss of accuracy, it can be considered additive and white. The noise contribution to every medical image pixel is unknown. however, it is possible to obtain the assessment of the entire noise contribution to the image from:

i) The standard deviation of the pixel intensity in a picture area, where the signal is relatively constant. Equation gives the formula used for calculating the standard deviation (SP):

$$\text{SD} = \sum_{i=1}^N \left[\frac{(x_i - \mu)^2}{N-1} \right]^{\frac{1}{2}} \quad (2.2)$$

Where, N: number of pixels involved mean intensity value xi: pixel value

ii) The noise power spectrum, which can be approximately assessed from the image high frequencies, as the S/N is small. If the image noise is considered white, then across the image's spatial frequency spectrum, the noise power spectrum is constant.

Finally, the overall image quality may be approximately evaluated by equation (3)

$$Image_Quality = \frac{(Sharpness)^2 (contrast)^2}{K \text{ noise_power_spectrum}} \quad (2.3)$$

2.3 INDICATIONS FOR CARDIAC CATHETERIZATION

As performed nowadays, cardiac catheterization is a combined hemodynamic and angiographic procedure performed for diagnostic and usually therapeutic purposes. As in the case of any invasive process, the decision of performing cardiac catheterizing has to be made on the basis of carefully balancing the risk of the process against the projected advantage to the patient. Indications for using catheterization and coronary intervention in managing ST-elevation myocardial infarction (MI), unstable and stable angina were defined by the “American College of Cardiology and the American Heart Association (37–39)”, a summary of the indications for the use of cardiac catheterization in patients that have stable angina. Concerning whether all patients that are considered for heart surgery need to undergo preoperative cardiac catheterization. A great deal of young patients with echo-proven valvular disease and without any myocardial ischemia symptoms are in some cases operated on the use of only non-invasive data, but the risks of catheterization in such Class I [17].

Patients that have increased-risk standards on the non-invasive testing irrespective of the severity.

Patients experiencing disabling (“Canadian Cardiovascular Society [CCS] class III and class IV”) chronic stable angina in spite of the medical therapy.

Patients that have angina and CHF symptoms and signs.

Patients that have angina and have survived serious ventricular arrhythmia or sudden cardiac death (SCD). Level of Evidence:

Patients that have clinical characteristics which show a high possibility of severe CAD.

2.3.1 Design of The Catheterization Protocol

All cardiac catheterizations must have a protocol, which means, a thoroughly reasoned sequential plan which is particularly designed for the particular patient. This protocol could be very common (for example, left heart catheterization with coronary angiography, annual transplant evaluation) which the operator and the support staff are already in synch with the plan. In the case of bleeding or bruising at the catheter site, in addition of <1 in 1,000 complication risk that requires emergency surgery. Or else, there is no necessity of going into complicated detail of every component risk, except for the case where the patient and his family require more details. The attempt is precisely stating the moderate amount of involved discomfort, the time of the procedure, and the post-procedure recovery—failure of doing so risks one's reliability. The practice is having the patient fasting (excluding the case of oral prescriptions) post-midnight, however, some labs permit a toast and light tea breakfast with no ill effects. Complete vital signs need to be recorded prior to the moment where the patient leaves the floor (for inpatients), or a short time after arriving at the Ambulatory Center (for outpatients), for the sake that the procedure could be reconsidered in the case where a change has happened in the condition of the patient since they have been last seen. As soon as the question of indications and contra-indications is dealt with, and the permission of the patient is acquired, the focus is directed towards the pre-medications matter [17].

2.3.2 Image Display and Processing

Before being displayed, digital images will be processed. Image processing approaches include grayscale transformations (changes contrast level), edge enhancement (which enhances the visibility of small structures that have high-contrast), smoothing (reduces the effect of noise in a single frame at the expense of image sharpness), and temporal averaging. This last function combines several image frames. It reduces noise while maintaining the sharpness of nonmoving structures. Digital video facilitates functions such as fluoroscopic last-image-hold and instant replay of fluoroscopic and cinefluorographic images. Reviewing stored images instead of continuing fluoroscopy is an excellent means of patient and staff dose reduction [21].

2.3.3 Flat-Panel X-Ray Detectors

The combination of image intensifier/camera is presently displaced via digital image receptors (flatpanel detectors) that are integrated with them. The indirect detector include charge-coupled device or photodiode visible light detector array in a direct contact with input phosphor. Both designs produce digital video signal with fewer intervening stages than described above for the phosphor image intensifier/video camera systems. illustrates structure of both dose efficiency regarding the flat-panel detector will be highly related to the efficiency of innovative image intensifier, therefore, the patient doses that are given through 2 fluoroscopes-the first a flatpanel and the second one an image intensifier- are going to be alike. Nevertheless, flatpanel fluoroscopic systems are usually of a wider dynamic range and more efficient dosimetric performance than older image intensifier-based systems owing to better dose management hardware and software in other parts of the fluoroscope. The imaging behavior of a flat-panel system differs from an image intensifier/ digital video system in one important respect. As shown in figure 2.5 when an image intensifier [17].

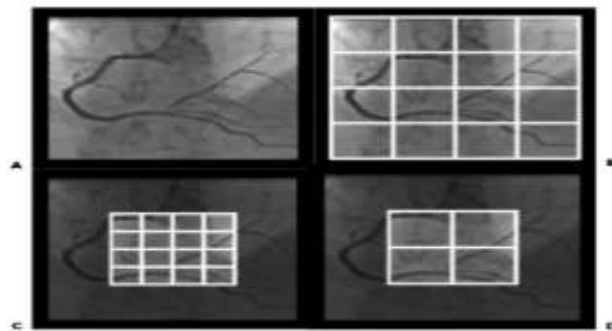


Figure 2.5: Zoom differences between image intensifiers and flat-panel detectors. The image before digitization (A); full-field digitization for both systems—typically a matrix size of 1,024 1,024 (B). When the image intensifier is zoomed (C), the same matrix covers a smaller field of view; this reduces the effective pixel size. When a first-generation flat-panel is zoomed (D), the pixel size remains the same; fewer

2.3.4 Cather

Doctors use catheterization for the purpose of detecting or treating coronary heart disease, which often causes heart disease and heart attacks, if not treated, because of its important role in providing the heart muscle to work properly. The catheter identifies and treats the blockages that occur in the blood vessels as a result of atherosclerosis. Cardiovascular sclerosis is often caused by the deposition and accumulation of blood plaques inside the artery, which obstructs the movement of blood towards it or prevents it from passing to and from the heart as in heart attacks. The catheterization is also performed in the case of a congenital heart defect to repair or reduce Damage caused by and it is shown in figure (2.6).



Figure 2.6: Cather

2.3.5 Prepare for Catheterization

Prior to undergoing the catheterization, the patient undergoes a number of tests including tests of stress, blood clotting, comprehensive blood test, and heart function planning. The patient's need for catheterization depends on the results of the previous tests. Suffers from one of them days before the catheterization and also abstains from eating or drinking and even smoking eight hours before the operation.

2.3.6 How It Works Catheter

The patient will be admitted to the hospital one day prior to the surgery to perform some necessary analysis and radiation. On the next day, the patient will be anesthetized locally to the thigh, arm or wrist, but usually the procedure is performed by the thigh. The patient is kept

awake during the operation, but the patient is given some intravenous medications to help relax him, and negative electrodes are placed on his chest, in order to monitor the heartbeat during the operation, and then The doctor works a small rip, then inserts a small tube, called the Qantar through the artery of the thigh, the doctor passes the tube into the main blood vessels until it reaches the coronary arteries in the heart, and in the process of cameras, especially Vascular, and then inject the doctor special material In the coronary arteries of the heart or in the left ventricle. Heart pressure is also measured, often in cardiac catheterization. D to keep the arteries open, and at the end of the operation the doctor breathes a small balloon, to open the closed arteries. The catheterization process does not mean that the patient's heart has fully recovered. However, some instructions should be followed to keep the heart healthy, such as avoiding smoking and alcohol, and reducing foods that contain High in fat and cholesterol.

2.3.7 Risks of Heart Catheterization

Risks of heart catheterization Infection in the surgical incision. Bleeding may be the result of certain medications. Risk of anesthesia, which is associated with hyperhidrosis in the person, and a drop in blood pressure. An injury to a blood vessel.

2.4 IMAGE ENHANCEMENT

The objective of this operation is improving the awareness of image information for the individual eye or providing a “better” input for other types of approaches of automated image processing. Image Enhancement (IE) converts images for the sake of providing a clearer representing of the sensitive details. Researchers consider it is one of the indispensable tools in many different areas, which include (but are not limited to) art studies, medical images, forensics and atmospheric sciences. It is considered to be application specific: an IE approach which is appropriate for one issue could be unsuitable for other problems. Forensic images or videos use approaches resolving the issue of low resolutions and movement blurring whereas medical imaging gets more benefit from increasing sharpness and contrast. In order to prepare for such a continuously increasing digital imaging demand, software companies presented commercial software for users that have the need of editing and visually enhancing images. The question that rises: Is the procedure of the manipulation of images, in a way that the results are better than original concerning certain applications? The word “specific” is of high importance in this subject, due to the fact that it decides at the beginning that approaches of enhancement are

problem oriented. Therefore, for instance, an approach which is rather beneficial for the improvement of X-ray images might not be the optimal methodology for enhancement of satellite images that have been captured in the infra-red band of the electro-magnetic spectrum. There isn't a general image enhancement theory. In the case of processing image for visual analysis, the spectator can be considered as the final reviewer of the degree of efficiency of a certain approach [22].

2.4.1 Approaches of Image Enhancement

Techniques of Image enhancement may be split to 3 main classes:

- 1-Frequency domain approaches that are operating on the Fourier transformation of images.
- 2-Spatial domain approaches that are operating in a direct manner on the pixels.
- 3-Fuzzy domain, unfortunately, there isn't a general theory that determines the definition of "good" image enhancement, as it relies on the perception of individuals. If it appears suitable, then it is good! On the other hand, when the approaches of image enhancement are utilized as tools for preprocessing for other approaches of image processing, quantitative measures may decide the techniques that are the most suitable [23].

2.5 FILTERS

In the case where images are transferred via channels, impulse noise could corrupt the images due to the noisy channels. Such noise includes large negative and positive spikes. The values of the positive spikes are considerably higher compared to background and thereby, they seem like bright spots, whereas values of negative spikes are considered lesser compared to background and those spikes seem like dark spots. Both types of spots are visible to the humans. Moreover, Gaussian noise also has an impact on the image. Therefore, before processing, filtering is required for impulse and Gaussian noise. Many classical and fuzzy filters are available for noise removal. The classical filters are adaptive Wiener, mean, the adaptive weighted, adaptive medial, weighted, Gaussian, the median, and the extended mean filters. The mean filter is helpful to processes of smoothing. It gets rid of the noise which is smaller in size or other small image fluctuation. It includes calculation of the mean values of brightness in a neighbourhood $m \times n$, after that it replace the grey-level with a mean value. This operation will blur the image and doesn't maintain edges. Those are not utilized to remove the noise spikes. For 3×3 neighborhood the convolutional masks.

$$\frac{1}{9} \begin{bmatrix} 1 & 1 & 1 \\ 1 & 1 & 1 \\ 1 & 1 & 1 \end{bmatrix} \quad (2.4)$$

Adaptive weighted mean filter (AWMF) can be considered like the mean in the fact that the grey level value is replaced via weighted mean of grey values. Weights are computed from the difference of the gray-levels. In the case where this difference is larger than a particular value of the threshold, after that the pixel will be considered as noise. Adaptive Weiner filter replace central pixel value by summation of local average value and fraction of contrast, as it is dependent on local variance estimate [24].

2.6 VIDEO ENHANCEMENT

During the past few decades, there was a notable amount of capability enhancement in Digital cameras, which include sensitivity and resolution. Those cameras are usually dependent on automatic exposure control for capturing high dynamic range images, however, usually, the longer time of exposure produces motion blur. Numerous methods have been established for the improvement of videos of low light; nevertheless, the majority of those methods consider videos from moderately dark conditions. In the presented study, a sufficient framework method has been proposed for the enhancement of videos from environments that are poorly illuminated, with the use of suitable approach of noise removal filter that maintains the quality of the image [25].

Digital videos have become an integral part of our daily lives. It is quite common that video improvement as a significant subject in computer vision has gotten a considerable deal of interest in the past few years. The objective is improving the visual quality of the video, or providing a “better” transformation representation for automated processing of videos, like detection, analysis, recognition, and segmentation. In addition to that, it is helpful for the analyses of background information which is of great importance for understanding behaviors of objects with no need for expensive human visual inspection. There is a number of applications in which digital videos are recorded, processed and used, like general identity verification, surveillance, civilian or military video processing, and criminal justice systems. More and more video cameras are commonly utilized in numerous cases, such as production Plants, Public places, domestic surveillance systems, and so on. The majority of those cameras operate in the open air, and that

indicates that the quality of videos is dependent on weather conditions. The systems of camera and video surveillance are projected to be of high efficiency in any weather and illumination condition, however, most of them have not been designed to operate in low-lighting, which is why, the low capturing quality of the video camera makes the video unsuitable for numerous applications in poor settings like pouring rain, dark nights, fog, and heavy snowing.

During the past few decades, there were considerable enhancements of capability in digital cameras, which included sensitivity and resolutions. In spite of those enhancements, modern digital cameras remain limited in taking images of high dynamic range in poor lighting conditions. Those cameras are usually dependent on automatic exposure control for capturing high dynamic range images, however, motion blur is produced by longer time of exposure. In addition to that, image sequences that are taken in bad lighting are usually of low SNR. In the case when the lighting is quite poor, the amount of noise become higher compared to signal, which is why, traditional approaches of denoising can't be used. For designing a sufficient and fast poor lighting enhancement of videos is a challenging issue. Numerous methods have been developed to enhance videos of poor lighting, nevertheless, the majority of those videos consider video from moderately dark conditions. In the presented study, the objective is developing an innovative framework for the enhancement of videos from very poor lighting conditions. The proposed approach includes temporal reduction of noise, denoising, and contrast enhancement.

The utilized software tool is MATLAB [25].The have proposed a method for noise elimination and adaptive enhancement for exceedingly dark sequences of images that are of quite low dynamic range[26]. The method is quite general, also it is capable of adapting to the spatio-temporal structure of intensity for the sake of preventing the blur that results from motions and smoothing across valuable structural edges. In addition to that, the approach includes a sharpening property preventing the most valuable object edges from getting over-smoothed. The majority of parameters may be defined for quite large set of input sequence. Those parameters consist of clip-limit in contrast-limited equalizing of histogram, maximal width and minimal width of filtering kernels and width of isotropic smoothing of the structure tensor and in computations of gradients. Nevertheless, the parameter of scaling for the function of width must be altered to the level of noise in the current sequence. The optimal methodology with the application of the approach to color images was discussed, and that included demosaicing from the Bayer pattern in raw input colored data in a simultaneous way to the reduction of noise. They have applied the approach with the use of a GPU and achieved interactive performance. [27]

proposed an innovative 3-stage algorithm for extremely poor lighting video de-noising and enhancing. A new model for de-noising and enhancing of very dark videos was proposed and has shown good improvement to the current state-of-the-art results [28] proposed a Kinect depth based approach for the enhancement of poor lighting surveillance images. Preprocessing for the Kinect depth map, depth constrained nonlocal means de-noising and depth aware contrast stretching are done in a successive manner, in the presented algorithm for promoting the visual quality for poor lighting surveillance images. Compared to older works, this approach is capable of enlarging the low dynamic range and simultaneously promoting local and global depth perceptions for poor lighting surveillance images. The experimental results have shown that this approach produces more distinct object edges and a clearer perception of depth for improved low-light surveillance image. High level of noise from low dynamic range and darkness are 2 features of poor light surveillance images which worsen visual quality. Presented an innovative model for enhancing very poor-light videos. For noise elimination, movement adaptive temporal filtering which is depends on Kalman structured updating has been proposed. Dynamic range of de-noised video has been enhanced via adaptively adjusting RGB histograms. Finally, the rest of the noise is eliminated with the use of a Non-local means (NLM) de-noising. The presented approach utilizes raw data of color filter array (CFA) to achieve low consumption of memory. Histogram adjustment with the use of the gamma transformation and the adaptive clipping threshold has been proposed as well for increasing low-light video dynamic range. The experimental results have indicated the fact that this approach has a great deal of potential for real time implementations to consumer cameras, particularly CCTV and video systems that are specified for surveillance. Is shown figure (2.7).

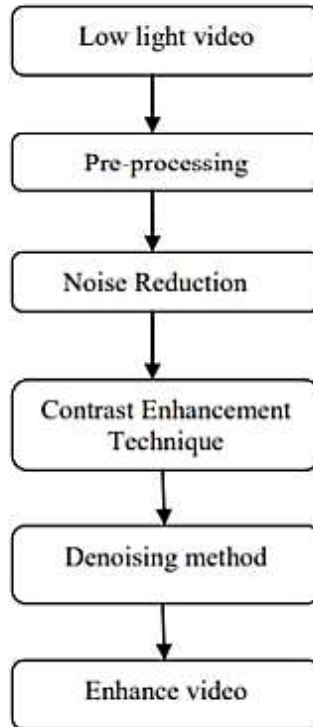


Figure 2.7: Enhanced video diagram

2.6.1 Preprocessing

The poor-illuminated video is applied on the 1st step, i.e. the preprocessing. Preprocessing is the term that is used for operations on images at the minimum abstraction level. Those operations don't increase the content of information of an image, however, they decrease it in the case where entropy measures information. The goal of preprocessing is improving image data which suppresses the unwanted distortions or enhance some image characteristics in video useful for additional tasks of processing and analyzing. Image preprocessing utilizes the redundancy in images. The poor lighting video is applied to the initial step, which is preprocessing.

2.6.2 Reduction of Noise

Noise results from errors in the process of image capturing, which result in pixel values which don't reflect the actual intensities of the actual scene. Due to the fact that sequences of images are temporally related, noise may be effectively eliminated via temporal filtering. Videos might

be subjected to different noise kinds. The result from initial stage is input to the noise reduction, which is the operation of eliminating noise from the signal.

2.6.3 Contrast Enhancement Methodology

Image contrast measures its dynamic range, or its histogram “spread”. The image’s dynamic range could be characterized as the entire scope of intensity values that are included in an image, in other words, it is the biggest value of the pixels - the minimal value of the pixels. Enhancements of contrast are responsible for improving the object perceptibility in the scene via the enhancement of the difference in brightness values between the objects and the backgrounds. Enhancements of contrast are usually carried out as a contrast stretch.

2.6.4 Self-Enhancement of Poor Quality Video

In the presented section, the emphasis is focused on poor quality videos self-enhancement. The methods may be categorized to 4 classes, which are: wavelet-based video enhancing, HDR-based enhancing of videos, enhancement of contrast, and compressed-based video enhancement.

2.6.5 HDR-Based Enhancement of Videos

HDR, i.e. the High dynamic range imaging can be defined as a group of approaches allowing a wider dynamic range of luminance between darkest and lightest regions of the image compared to the traditional approaches of digital imaging or photographic techniques. The increased dynamic range enables HDR images of more particularly representing many levels of intensity in the actual scenes, which range from direct sun-light to faint star-light. Nevertheless, as shown figure 2.8, the dynamic range in actual environments.

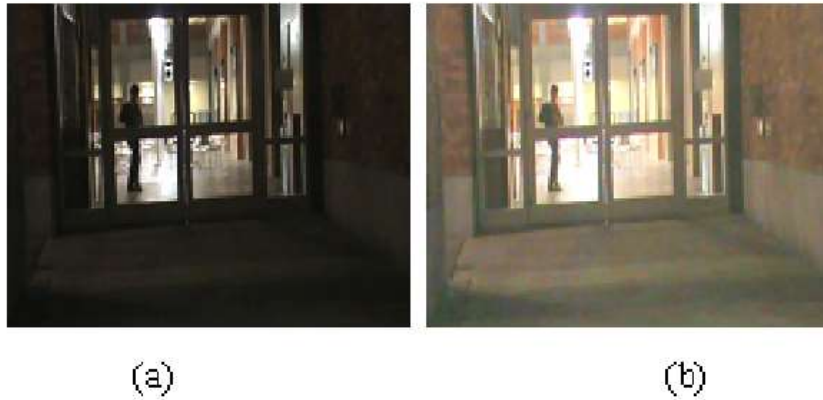


Figure 2. 8: (a) Original night-time video frame, (b) Improved night-time video uses tone mapping approach [29]

Therefore, far exceeds the range which has been denoted in 8bit/channel maps of texture. Extended dynamic range may be obtained via a combination of numerous images of one scene which has been captured with various, known times of exposure. The output is a radiance map of floating points with radiance values that are proportional to the ones that are seen in the actual scene. The 2 fundamental HDR imagery sources are computer renderings and combining several photos, and that, in turn is referred to as LDR , which means low dynamic range [30].

Videos are capable of encoding higher contrast or dynamic range. HDR video and image formats are modeled for encoding each luminance level which could differ from cd/m^2 (moonless sky illumination) to cd/m^2 (sun light). Like the HDR imaging, there is a number of various ways for obtaining HDR video, which includes capturing HDR images with the use of video cameras, adaptive light modulator, fixed mask, and differing alternate frame exposures. HDR videos use tone mapping across frames for converting floating points to the 8-bit representations in order to render in the standard monitors. Based on the human visual system model [31], proposed an innovative definition of visible distortion based on detecting and classifying perceptible variations in the structure of the image. Which is why, merging varied exposure frames approaches is desired. There is a number of approaches for obtaining the groups of frames to be used in the generation of radiance maps, and result in a trade-off of the spatial or the temporal resolutions. In the formatting process of HDR video for displaying, frame by frame mapping of

tone is not suitable, as changes in the values of luminance across frames may produce artifacts, therefore, the solution is using temporal tone mapping.

In addition to that, there is a wide variety of approaches for temporal tone mappings that take under consideration values of global or neighboring frame luminance, every one of them with associated benefits and drawbacks. What is the way to improve the enhancement of videos? A summary of a group of the approaches in those classes are:

A) Radiance maps for generating HDR images from a group of LDR images, an algorithm is needed for combining and precisely mapping the relative values of luminance for images. The resulted map from the values of luminance is referred to as the radiance map, this map could include values ranging over numerous magnitude orders, based the group of exposures. The main problem in implementing the generation of radiance map is the nonlinearity of capturing devices. Throughout the process of scene capturing, the actual values of relative luminance that are recorded and saved by the device have no linear correspondences, for example, in the case where a point in the scene has a value which is two times the luminance of some other point, the value of luminance of the brighter pixel might not be inevitably two times the value of the darker pixel. This nonlinearity makes the procedure of merging photos of a higher difficulty. For the sake of resolving this problem [32], used the sensor reciprocity constraint for deriving the values of response function and relative radiance in a direct way from a group of images that have been captured with various exposures. The algorithm might merge numerous photos in one. The radiance map of HDR of pixels values are proportionate to actual values of radiance in scene. To alter illumination for new adding objects [33].

B) HDR-based context improvement video image quality enhancement approaches result in impressive accomplishments due to the fact that devices of display are rapidly progressing. Nevertheless, there are a few drawbacks on intensity representation of devices of displaying and acquiring for reproducing the video images of real world. A variety of context-based approaches of contrast enhancement were advanced and applied for overcoming this set of issues on representation of intensity of display and capturing devices for reproducing real world videos. Nevertheless, there remains a number of limitation, which include lighting information loss, changes in color information, and excessive enhancements. For resolving those issues [34].

C) HDR-based lighting enhancement: HDR output video cameras are specifically appropriate for driving applications of assistance, in which illumination conditions might considerably range from direct sun-light to dark places such as tunnels. On the other hand, typical devices of

visualization are only capable of handling a low dynamic range, and therefore, there is a need for a dynamic range reduction. A number of algorithms were suggested in for reducing the dynamic ranges of static images. Some of the existing approaches to videos aren't direct for reducing the dynamic range of static images, because of the peculiar nature of video data [35].

2.7 ABOUT THE NEXT CHAPTER

In our thesis, we will use the practical side of the next chapter. The algorithm consists of three axes. The first path is the method of improving the enhancement the video floor and the second path is the method of improving enhancement the video and third path enhancement the Image We will explain these axes.

2.8 VIDEO FRAME BEFORE ENHANCEMENT

In particular scientific experiments it is sometimes needed to combine captured static image sequences for reconstructing the system dynamics and observing the way of system behavior throughout time. In case of the extraction of protein dynamics from several samples, each of which has been damaged post measurement, it is corresponding to reordering a video that had its frames randomly shuffled. The suggested algorithm utilizes feature based matching for determining the distance between frames and proposed two sorting algorithms for frame reordering with taking under consideration the metrics of computed distance. Utilizing those approaches, the algorithm accomplishes efficient reconstruction of two-dimensional videos[79].With the rapidly increasing size of video data, compact video representation is keeps gaining importance and attention for sufficient communication and browsing that results in a number on video summarizing in the past years. Amongst those works, summaries depending on a group of static frames are commonly researches and utilized because of their high compactness. Nevertheless, representativeness of the chosen frames that have been considered as compact representations of videos or video segments, have not been deeply researches. It has been noted that representativeness of frames is tightly correlated to some elements, which are: quality of the image, visual details, measure of user attention, and duration of displaying. It has also been noted that users similarly tend to select the most representative frame for a particular segment of video developed an approach for examining and evaluating the video frame representativeness based on learning users' perceptive evaluations [80].

2.8.1 Representativeness Learning

It has been noted that video frame representativeness is associated with the some elements, which are: Frame Quality (fF Q): evidently, poor-quality frames are unsuitable to represent a segment or a video. Increasing the quality, will make the frame more representative. Quality of the frame includes: frame contrast and clearness. Entropy is a good measurement for the contrast of an image greatly determining image quality. Concerning the clearness of the frame, its opponent will be used to measure it, which is frame blur that includes blur which is resulted from defocus and motion. Calculating defocus blur has been discussed in [81]. While motion intensity of a camera, MI (Subijk), which is computed while sub-shot is obtained in Section2, gives rough measure for movement blurring.

Visual Details (fVD): this measure reflects whether scene or object details in a frame are clear enough. For the sake of evaluating image visual details with no reference (literally, blind image evaluation), level of the sharpness of the edge [82] has proven useful and easy to implement. Content Dominance (fCD): concerning the dominance of content, frame stableness has been used for measuring it. Due to the fact that those two measures are related in the fact that the slower is the movement of the camera, the higher is the stability of the frames, and the greater is the dominance of the content is in the video segment. Stableness has been calculated via averaging of the frame histogram differences between current frame and adjacent five that are before it and following it.

Attention Measurement (fAM): it has been presented in [83] is has been found rather relevant with frame representativeness in video segments. Due to the fact that the more a frame is attractive to the viewer, the more likelihood there will be that it is selected as the video segment representative. In addition to those characteristics which are shared in measures of representativeness of subshot, shot and scene, for measuring of representativeness in subshot, the location of every one of the frames in the segment (fPS) needs to be added. And for shot, there are some other characteristics, like: subshot duration (fSD), camera motion types (fTY), and neighbor subshots durations (fND). And for measure of representativeness in a scene, shot duration (fSD), frame similarity (fSIM) and so on need to be added. Every one of the samples in a subshot, shot, and scene may be denoted by its multidimensional feature vector like:

$$f = [f^{(1)}, f^2, \dots, f^{(d)}]^T \quad (2.5)$$

Model representativeness measurement in the feature space. After that, the task become a problem of supervised learning. In fact, the representativeness measurements of frames that are neighboring to most representative (MR) frames are usually near the ones of MR frames. Which is why, approaches of discriminative learning, like SVMs are unsuitable in this case, due to the fact that it is inappropriate regarding each one of the non-MR frames as negative samples. Therefore, an approach of generative learning needs to be applied, which attempts at modeling the MR frame distribution. It should be postulated that the idea of “representative” has a finite mix distribution in feature space X , denoted as:

$$R_x(x|\theta_k)=\alpha_m N(\mu_m, \sigma_m) \quad (2.6)$$

k represents the number of Gauss components $N(\mu_m, \sigma_m)$. $\theta_m = (\mu_m, \sigma_m)$ represents the average and co-variance matrix, in addition to value of α_m .

2.9 EXTRACT MOVIE FRAMES

Video summarization is one of the main tasks in the algorithms of video analysis and indexing. Extraction of video key frames. This process is a key procedure for retrieval and summary of videos. The new proposed method is based on interest points description and repeatability measure. Prior to extracting the key frame, the video must be divided to shots. After that, for every one of the shots, interest points are detected in every image. Video summarization aims at reducing the amount of data which needs to be tested for the sake of retrieving certain information from a video. It is one of the most important steps in video indexing, archiving, and retrieval. With the latest enhancements in video applications, a considerable amount of researches was performed on content-based video retrieval and summary. An innovative method will be presented for extracting visual summary of a video data-base, which will be constructed by the key frames that have been obtained from the video data-base. The user might start their query via choosing one image from the visual summary which has been presented. Every one of the videos from the data-base is going to be presented by some key frames. It considerably decreases the amount of data which needs to be examined via providing a brief and precise video representation. The aim of key frame extraction is converting the whole video to a small number of representative images maintaining the salient video content [83].

2.9.1 From Video to Image

Object motion presents relative shift (in pixels) regarding the regions between succeeding instant images $\tilde{x}(t)$. considering maximal shift Δ which is to be handled, and via determining negligible blur as shift of one pixel, it becomes possible defining the maximal number T of time segments via making $T = \Delta$. This option merely makes sure that on average every one of the frames $x[i]$ is not going to have any motion blur. On the other hand, motions with acceleration could result in blur which is larger than one pixel in some of the frames. The model of motion-blur (1) therefore far defined is rather general, as areas might shift in an unconstrained manner and successive instant images might present or eliminate texture (occlusions). However, such framework is capable of handling the most general motion-blur cases, which is typically referred to as the dynamic blur. Which presents a new design of movement de-blurring with dynamic blur: taking a movement-blurred image y , recover the T frames $x[1], \dots, x[T]$ satisfying model. Like it has been stated in the Introduction, the task of enhancing a sharp image from a blurry image is usually very poorly formulate. On the other hand, in the light of the obtained formulation, the level of the challenging of task gets more difficult by the loss of the ordering of the frames in the model. There can be a possibility of determining the local ordering of successive frames via applying temporal smoothness, nevertheless, there are numerous ambiguities which have been described and discussed in the following section. For instance, given y it is not possible knowing whether the ordering of the original sequence was $x[1], \dots, x[T]$ or $x[T], \dots, x[1]$, and that represents all objects that move forward or back in time. Because of the complexity of the task, a data-driven method has been adopted. A data-set of blurry images has been built with corresponding ground truth frames with the use of videos that are of high frame-rate as in latest approaches, and devise an innovative training approach with convolutional NNs (as in Sec. 5.3). which predicts a blurry result which represents the average of the possible options. There's an exception to those vagueness. The central frame in a sequence of odd-number doesn't vary over the four instances. Which clarifies the reason why previous approaches were capable of successfully training an NN for predicting the central frame. For addressing the temporal order in ambiguities innovative loss functions have been introduced. In the following different options are explained, in addition to explaining the way the proposed loss function has been obtained. Those cases will be examined and evaluated as well in the section of Experiments. Covariance as a structural measurement of similarity for the block of image x , y of the correlation coefficient, which is the covariance of x and y , is calculated as:

$$\sigma_{xy} = \frac{1}{N-1} \sum_{i=1}^N (X_i - \mu_i)(Y_i - \mu_i) \quad (2.7)$$

In this equation N denotes the number of patches and μ_i is the mean value. In the substitute sequence of the key frame.

Blocks at the same index (in the initial image) and (in the testing image), the structure similarity component between the two image block sis calculated as (x,y) :

$$S(x, y) = \frac{\sigma_{xy} + C}{\sigma_x \sigma_y + C} \quad (2.8)$$

Where $C = ((KL)2/2)$, $K \ll 1$, $L \in (0,255]$ and σ_x , σ_y are x and y variance, respectively. In the case where the component values of (x, y) are small, then the difference between information contents is not; also, they do not necessarily need to be kept as a key frame that may be obtained only while a key frame is enhanced [84].

2.10 THE FIRST METHOD (RETINEX)

Retinex Theory has been first proposed by E. H. Land in the year of 1964, also additional development of “reset Retinex” which is formulated via Land and McCann. It has been the original effort of simulating and explaining human visual system (HVS) of the way of perceiving color based on experiments with the use of patterns of Mondrian. Progressively, a number of Retinex algorithms were developed and utilized to several imaging fields. Retinex algorithm is an algorithm of image enhancement which depends on the approach of illumination compensation. It presents explanation of the color constancy and contrast phenomena where it considers that perceived object colors are mainly invariant to chromaticity of the light incident upon them. It was attempted discussing here a review on retinex algorithms basics and briefly showing the way there’s change in the enhancement of conventional retinex algorithm that modifies the entropy its mean gradient, standard variance indicating the fact that the images include more information and details of original images.

2.10.1 Retinex Theory

Retinex is the process by which an image is automatically provided with visual realism. Its name comes from the combination of words, "retina" and "cortex", which suggests that each of the brain and eye are take part in processing. The theory of Retinex has been motivated by Land[36] it was based on the model of physical imaging, where image $I(x,y)$ is considered to be the result

of multiplication: $I(x,y) = R(x, y) \times L(x,y)$ in which $R(x, y)$ is the reflectance and $L(x, y)$ is the lighting at every one of the pixels (x,y) . in this case, the nature of $L(x, y)$ is characterized with the source of light, while $R(x, y)$ is regulated by the properties of the objects of the image. Which is why, the normalization of illumination may be performed via the estimation of the lighting L and after that dividing image I by it. Nevertheless, it is not possible estimating L from I , unless some other detail is known concerning L or R . therefore, a variety of presumptions and simplifications concerning L , or R , or both are presented for solving this issue [37]. One of the popular assumptions is that edges in a scene are reflectance edges, whereas lighting could spatially and slowly change in a scene. Therefore, in the majority of Retinex approaches, the reflectance R is calculated as ratio of I and its smoothed version that plays the role of lighting estimate L , and several smoothing filters for the estimation of lighting were presented. Retinex theory chiefly compensates for the effect of images that are impacted by lighting [38]. according to image formation model of Retinex:

$$S(x, y) = R(x, y).L(x, y) \quad (2.9)$$

The retinex formula is $S = RL$, $S \in [0, 255]$ represents the spotted image, $R \in [0, 1]$ represents reflectance and $L \in [0, 255]$ is the lighting. It is a difficult issue solving R and L with the use of one of the observed images S , therefore, other assumptions need to be adopted for constraining this issue. The following known information is utilized as constraint of the presented model: 1) lighting is spatially smooth; 2) R value ranges between 0 and 1, indicating that $L \geq S$; 3) the reflection includes a part of high frequency, in other words, information of edge and texture. Algorithms of Retinx are converting the input image to Logarithm domain. As presented in eq. 2:

$$\log S = \log R + \log L \quad (2.10)$$

Thus, as depicted in equation 3, the reflectance logarithm may be obtained by the image logarithm the illumination logarithm.

$$\log R = \log S - \log L \quad (2.11)$$

After that, the reflectance may be achieved via taking its index form, as depicted in equation4.

The reflectance is inherent characteristics of the actual object.

$$R = \exp(\log S - \log L) \quad (2.12)$$

Due to the fact that the lighting compared to the reflectance is a component of low frequency, thus, Retinex Algorithm utilizes low-pass filter for estimating the component of illumination. [39] this algorithm can be categorized to 3 types: path-based, recursive, and center/surround algorithms. Single Scale Retinex (SSR)[40] algorithm is the first one of the presented center/surround algorithms which are capable of either achieving compression of dynamic range or rendition of colour/lightness, but not both in a simultaneous way. The compression of dynamic range and rendition of color/lightness have been combined by the algorithms of Multiscale Retinex (MSR) and Multiscale Retinex with Color Restoration (MSRCR) [41] with universally applied restoration of colors.

2.10.2 Image of Classification

SSR Algorithm: The fundamentals of this algorithm consist of a logarithmic function of photo-receptor which is capable of approximating vision system according to a center/surround [42] function. This algorithm is represented by the following formula:-

$$R_i = \log_i(x,y) \log[F(x,y) \times I_i(x,y)] \quad (2.13)$$

The aim of logarithmic manipulations is transforming a ratio at pixel level to an average value for wider area. The representation of center/surround retinex pays a resemblance to the function of Difference-of-Gauss (DOG) which is commonly utilized in natural vision science for modelling each of the receptive fields of particular neurons and the perceptual procedures. The only needed extensions are a) considerably enlarging and wakening the surround Gauss (as given by its constants of space and amplitude) and b) including a logarithmic function for the sake of making subtractive function inhibition in order of making subtractive inhibition to a shunting inhibition to a (in other words, arithmetic division). The function of the surround space calculates the mean value of the values of the adjacent pixels and allocates it to the middle pixel. [41] has presented an inverse square spatial surround function:

$$F(x,y) = K * \exp\left(-\frac{r^2}{c^2}\right) \quad (2.14)$$

Moore has presented the exponential equation with absolute parameter:

$$F(x,y) = K * \exp\left(-\frac{r}{c}\right) \quad (2.15)$$

Hurlbert suggested:

$$F(x, y) = K * \exp\left(-\frac{r^2}{c^2}\right) \quad (2.16)$$

For a certain space constant, inverse-square surround function to which greater response is attributed from surrounding pixels compared to exponential function and Gauss function. The spatial response of exponential surround function has been greater compared to the special response of the Gauss function at distant pixels. which is why, inverse-square surround function has been more widely utilized in the compression of global dynamic range and Gauss surround function has been utilized, in general, in the compression of the regional dynamic range [43]. The exponential and the Gauss surround functions have been capable of producing sufficient dynamic range compression over the surrounding pixels. Selecting the space constant is associated with the visual angle in direct observation. However, the value can't be modeled and determined theoretically. Mainly, there's a compromise between dynamic compression, (for instance, details in shadows) and colour rendition. SSR is not capable of the simultaneous provision of efficient compression of dynamic range and tonal rendition. In addition to that, it introduces halos surrounding the objects. The function returns the "illumination invariant" reflectance R and the projected function of luminance L (each of them is in the domain of the log). In this case, the function of luminance is returned for purposes of visualization only, due to the fact that it is typically not of a great value from the viewpoint of lighting invariant facial identification.

A. SSR Features

Generally, SSR has the following characteristics -

- The location of logarithmic function is following surround formation.
- The functional representation of the surround is Gauss.
- A tradeoff exists between tonal rendition and dynamic range Compression which is regulated by Gauss constant of surround space. A space constant of 80 pixels is an adequate trade-off between the dynamic range compression and the rendition.
- The post retinex signal processing is a canonical gain off-set instead of an automatic gain off-set.
- Violations of the assumptions of gray world produced retinex images that have either been greyed out locally or globally or more seldom had the issue of color distortion.

. • A single scale appears to be unable to simultaneously provide adequate tonal rendition and dynamic range compression.

2.10.3 Multiscale Retinex Algorithm

For the sake of preserving color rendition and dynamic range compression, MSR, represented in combination of weighted different SSR scales [44], is considered to be an efficient solution. The new MSR algorithm for enhancing medical images on the basis of multi-rate sampling was utilized as well. The speed of this algorithm has been greatly enhanced, due to the fact that the various sampled versions of value channel are processed in parallel. The fundamental practical result of this is that Multiscale retinex is unsuitable for applications that are color-sensitive. In the context of image processing/ enhancing, Multiscale retinex plays the role of a sub-set of the following 4 image processing objectives, according to the situations:

- a. the compensation for un-calibrated devices (i.e. gamma correction)
- b. Dynamic range compression
- c. Color constancy processing
- d. Colour enhancement component of the n-th scale, W_n is n-th scale weight. For Multiscale Retinex, the number of required scales, their values and their weights are of considerable importance. Experiments showed that 3 scales can be sufficient for the majority of images and weights could be equal. In general fixed scales of 15, 80 and 250 might be utilized, or fixed portion scales of image size may be utilized. The weights may be altered for weighing more on color rendition or compression of dynamic range [45]. The Multi-scale Retinex based images have considerable compression of dynamic range in the edge between light and dark parts and sufficient colour Lenka et al., "International Journal of Advanced Research in Computer Science and Software Engineering 6"(1), rendition in the entire image scale. MSR included a combination of different weightings of SSR, choosing the number of scales that are utilized for the application and the evaluation of the number of scales which may be fused.

Important problems should be taken under consideration were the number of scales and scaling values in the surround function, and the weights in the Multi-scale Retinex. The optimal weights needed to be selected for the sake of obtaining proper compression of dynamic-range at the edge between image light parts and dark parts, and for maximizing the rendition of brightness [46] over the whole image. Multi-scale Retinex operated by compensating for changes in light for

approximating the human perception of an actual scene. There have been 2 approaches for achieving this:

(1) Comparing the psycho-physical mechanisms between a captured image and the visual perceptions of humans of an actual scene, and (2) Comparing the acquired image with the values of measured reflectance of actual scene. Which is why, the approach included combining certain characteristics of MSR with SSR processes, where the center/surround operation has been a Gauss function. After that, the logarithm has been utilized post the processing of the surround function (in other words, 2-D spatial convolution). After that, suitable values of gain and offset have been found based on the output of retinex and histogram characteristics. Those values have been constant for every image. This process resulted in the MSR function. Nevertheless, it is hard predicting if the reproduction color is going to be precise; it has color sensitivity problems [47]. This is not considered true for other adaptive methods as well, due to the fact that lighting variations might result in control parameters variations. For the sake of overcoming the error in MSR in colour processing MSRCR is followed.

2.10.4 MSR with Colour Restoration (MSRCR)

For reducing the computational complexity the 2-D filtering between image function and surround function will be done in frequency domain via calculating the result of multiplying the spectra of two functions.[48] The issue with MSR regarding restoration of the color, in which weights are given for 3 color channels according to the relative intensity of the 3 channels in initial images. In images violating assumption of grey-world, which means that images in which a particular color could be dominating, the procedure of MSR retinex generates grayish images via diminishing the saturation of the color. For solving this issue, Jobson et al. [49] suggested completing the algorithm with a step of color restoring. They have suggested modifying the result of the MSR via multiplying it by a function of colour restoration of the chromaticity. The initial step is computing the chromaticity coordinates Individual the relative intensity of 3 channels is given. Due to the fact that fidelity of the colour in image reproduction is complicated and active area of study, therefore it is assumed that the change in intensity has no impact on the aspects of perceived non-intensity of the colour. But merely an approximation. Even for separate colors, the appearance of the color changes with intensity. In addition to that, it has been found that the original MSR also presents no solution to those issues, and the altered MSR version is the MSRCR which is better suited for the addition of deviation corrections from every

assumption and for including more complicated appearance models of colors, which includes models for simultaneous effect of contrast.

The algorithm of MSRCR is commonly utilized in compensation of illumination. This issue might be addressed with the introduction of weight factor for a variety of channels in MSR with color restoration (MSRCR). It is helpful for overcoming the issue of color constancy to some extent. Color constancy that indicates computational methods for recovering the real color of the surface objects irrespective of light source color. Color is of high importance in a variety of applications like human computer interaction, extraction of color features and models of color appearance. The light source color has a considerable impact on the object's color in the scene. Therefore, this very object, captured via same camera yet in another illumination, could differ in its estimated color values. This variation in the color could result in negative impacts on the digital images. Humans have the capability of recognizing the real color of an object in spite of the variations in the light source colors. This issue is solved by introducing weights for 3 color channels according to the relative intensity of 3 channels in original images [50].

$$C_i(x, y) = f[I_i(x, y)] \quad (2.17)$$

The relative intensity of 3 channels is:

$$I_i(x, y) = I_i(x, y) / \sum_{i=1}^s I_i(x, y) \quad (2.18)$$

The function of the color restoration needs to be monotonic. As s represents entire number of colour bands which is 3. Numerous linear and non-linear functions have been applied; Jobson has discovered that the optimal overall restoration of the color was:

$$C_i(x, y) = \log[I(x, y)] \quad (2.19)$$

This approach of color restoration may be represented as:

$$RMSRCR_i(x, y) = C_i(x, y)RMSR_i(x, y) \quad (2.20)$$

Where $RMSRCR_i$ represents the i -th band of the result of the MSRCR. The equation above provides an idea concerning a general method for the algorithm of MSRCR. For improving this approach some alteration in the algorithm is performed. Sometimes FFT is applied as well. From the research, it has been discovered that the original MSR does not solve those issues as well, and that the proposed newer version of MSR is the MSRCR is better suited for the addition of deviation corrections from the assumption that is mentioned above. Therefore, it is

acknowledged that a valuable topic for future works will be to include more complicated models of color appearance, which include models for simultaneous contrast as it has been discussed previously. Sometimes it is projected that an approximation of faithful reproducing of the colors is utilized for preserving factor of chromaticity, as stated by the following equation.

$$X = \frac{x}{x+y+z} \quad (2.21)$$

Assuming that the reproduced chromaticity of a region X' , Y' , is matching to scene chromaticity of region X Y , then it immediately follows.

$$X = KX, Y = KY, Z = KZ \quad (2.22)$$

2.10.5 Retinex Operators

The initial work by Land and McCann [51] included a description of 4 stages for all iterations of Retinex computation, those steps are: ratio, product, reset, and average.[52] all operators, except the reset,[53] have stayed the same throughout the years. Those operators are used to the image in an iterative way, but the manner by which they are applied has changed. The emphasis of this study has been focused on listing the details of the way those 4 operators are utilized to the image.

One of main concepts behind Retinex lightness calculation at a certain pixel is comparing the pixel's value to other pixels' value. The major difference between algorithms of Retinex is how other comparison pixels are selected, and that includes the order by which they are selected. They utilize similar computations, yet they have greatly different computational in managing large real images. The initial manner of comparisons is via following group of paths or a path, from a pixel to an adjacent one through the image.[51] Estimate of lighting are gathered along the path in sequential product $\sim SP!$. SP begins as 1 and after that is multiplied with ratio of following pair of pixels along path. When the path following, the length of the path greatly impacts the results. Short paths indicate that the comparing is done only to others in a spatially localized set of pixels. Lengths of intermediate paths need to be utilized in the case of modeling the vision of humans. Infinite lengths of paths produce a degenerate case, where the resulted image is simply a scaled. A reset step is a second important characteristic of Retinex. Whenever a comparison is done, SP needs to be tested; in the case where it is bigger than 1.0, its value is reset to 1.0. here, the value 1.0 becomes the current estimate of lightness. A 3rd Retinex aspect is how estimates of lightness that are obtained from various paths to a pixel are combined. In older versions, Retinex included a step of thresholding as well. Nevertheless, it hasn't been included in

newer versions[54] and it isn't part of the MATLAB implementations that have been shown later. The 4th step finds the average of the present product values with preceding product values.

2.11 WAVELET TRANSFORM (WT)

The idea of the Muweiji conversion dates back to 1807 in his theory of Iterative Analysis, now known as Fourier Transform, which was the basis for the first idea of the Haerian conversion of the researcher Haar in 1909 in his thesis through the use of functions. After 1930, a group of researchers began to study the concepts of basic functions and the variable variable core functions called the basic Haar, which were the key to understanding the theory of Moji conversion. This research resulted in an effective algorithm To conduct digital bass image processing. The Moiji transformations have advantages and properties that rely on statistical guesses, which play a large role in digital processing, which researchers have helped to use in many applications, and the fact that it analyzes the signal, or the image to multiple levels of detail. And clarity in both the temporal and the temporal domains, which is one of the most important characteristics used in the strengthening of the edges of digital images. The waveguide gives strength in analysis compared to Fourier transform because it represents a variable analysis in terms of frequency window division over time, Make it fit. For many applications, as well as its advantage in the multiresolution analysis method, where the images are treated through the details resulting from the analysis of the image to several levels, and to a number of sub-images, Al Muwaiji is a practical application directly on the digital computer is an important application in digital image processing field [55].

2.11.1 Applications of Wavelet Transform

The theory of Moji conversion is one of the advanced theories presented as an alternative to Fourier transform, having its own self-similarity, as well as its ability to represent Multi resolution Analysis, making it an effective tool in numerous applications like sound compression techniques, Image, Computer Vision, and Computer Graphics. The standard tool in signal and image processing applications has become the standard tool because of the wide range of processes and functions that can transform the waveform from its representation, as it is an excellent tool for data compression (Data Compression, remove the The application of waveguide conversion technology in the analysis of several types of signals, such as radar signal, seismic signals and digital images, is the best choice because of its potential in the analysis of phenomena (Non Stationary Phenomena) [56].

2.11.2 Properties of Wavelet Transform

The advantages and characteristics of the Moji conversion have been identified in most applications, making researchers use it as a new tool, effective technique, and powerful in signal representation [58] and analysis. These characteristics are as follows [59]:

a. The Moji transfer gives information about the location in both the temporal and the temporal domain [57], [58], [59].

b. Molecular conversion allows separation of signal compounds in both time and frequency.

The waveguide has a great advantage in progressive transmission compared to other common methods. In addition to its high efficiency in the process of compressing, the process of retrieving the image data is represented hierarchically. Therefore, the image retrieval process of the images is very suitable for compression Successive images.

d. The number of processes needed for achieving waveform conversion is proportional to the length of the signal in an instantaneous transformation. Figure 2.9 shows the frequency-to-time division of time for this conversion.

e) Analyzes the signal or image to multi-resolution analysis in the time and frequency fields, as shown in Figure 2.10. This characteristic is one of the most important characteristics used in satellite data processing and data.

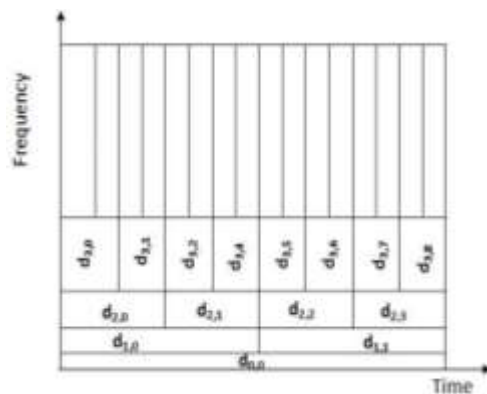


Figure 2.9: Molecular conversion representation (frequency division to time) [57]

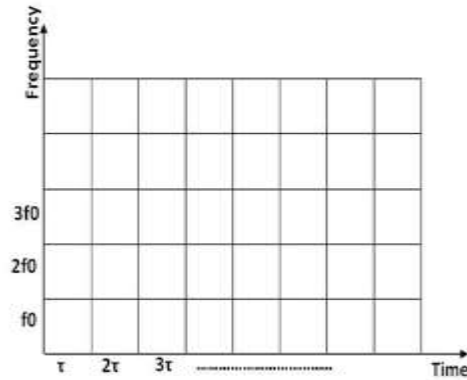


Figure 2. 10: Fourier representation (frequency-to-time division)[59]

2.11.3 Edge with Wavelet (Strengthen the Edge with Wavelet)

The purpose of strengthening the edges of image is highlighting the exact details of that image, or to further improve the blurry details resulting from the image processing, as in the images retrieved after the compression process of detail information is in the high-frequency vehicles in the image so most technologies The edges of the image are strengthened on some high-moving mechanisms. The process of strengthening the edges in the Muji space is accomplished without the need for a high-pass filter. The precise details are rough edges In a (LL, HL, LH, and HH), which means low (low) for LL, HL, LH, and HH. (Low-high) for LH and (high-high) for HH by multiplying it with a Amplification factor (Ratio) and its value is greater than one when we want to amplify the details, From 1 when we want to make the picture confusing[58]. Since the values of the Mujiia analyzed image variables vary from one level to another, the use of the same amount of amplification factor value will result in unbalanced inflation at the edges of the image. This problem can be addressed by giving a variable (decreasing) value for each package of analysis,

A mechanism has been proposed for the determination of the variable values of the amplifier based on the use of Decay because the multiplication process with the amplification factor can result in a decrease in coefficients when moving from a smooth to a higher level. If the decay factor is less than One that will reduce the potential The latter factor, which will reduce the

amplification edges in the details of the analysis of the level of the soft top value of the process, and after the completion of the strengthening of the edges on the image conversion process, the enhanced image is retrieved by using the reverse conversion wavelet process [60].

2.11.4 Mathematical Expression for Wavelet Transform

The wavelet is constructed from fully defined functions in space time, and functions defined in time are defined as functions that take non-zero values within the given period and take a value of zero outside the given period. the primary wavelet (mother wavelet), either by Shift or Scale, and each of the scaling or standardization changes a form of the parent wavelet, but in a controlled manner, so the original shape of the mother-wave can be restored again as it comes [61]:

$$\psi_{a,b}(t) = \frac{1}{\sqrt{a}}\psi \times \left(\frac{t-b}{a} \right) \quad (2.23)$$

a: Dilation Factor, or Scaling Factor, not equal to zero.

b: Translation Factor, or Time Delay.

Ψ : Mother Wavelet.

When displacement coefficient $\in L2 (R)$ is the parent wavelet, and $L2 (R)$ is the function space. ($A < 1$), the wavelet will be short and will be accompanied by low frequencies The waveguide equips an analysis of the time-frequency (or frequency-standard) level [61].

2.11.5 Types of Wavelet Transform

Wavelet Transform-WT is divided into three types based on the type of functions that are being utilized, and by the nature of the input function to this conversion, and the division is as follows [62]:

- CWT-Wavelet Transform Caller.

- Semi-intermittent waveguide (SDWT- (Sub- Discrete Wavelet Transform- SDWT)

- DWT This type of waveguide is known to have no integrations or derivatives, but only multiplication and collection, making it suitable for use on digital computers. This analysis is carried out by the following formulas[63]:

$$d_{j,k} = \sum_{n=-\infty}^{\infty} X(m) * \Psi_{j,k}(m) \quad (2.24)$$

The coefficients ($d_{j,k}$) are known as approximation Coefficients, m is known as the Scaling Function, $d_{j,k}$ is represented as Detail Coefficients, The wavelet function obtained from eq. (2.24) [63]:

$$\Psi_{j,k}(m) = \sqrt{2^j} \Psi(2^j m - k) \quad (2.25)$$

In the same way, the change function is obtained from eq. (2.25):

$$\Phi_{j,k}(m) = \sqrt{2^j} \Phi(2^j * m - k) \quad (2.26)$$

Wavelet Categories [64][65]

A. Haar Wavelet

One of the plainest categories of Mujajah, and is expressed by the following formula:

$$M_k = \begin{cases} \frac{M}{2^k} & 1 \leq k \leq N \\ \frac{M}{2^N} & k = N + 1 \end{cases} \quad (2.27)$$

B. Daubechies Wavelet

In contrast to Ingrid Daubechies, she invented the so-called orthodontic orthogonal orthopedics (Compactly Supported Orthonormal Wavelets), thereby making the intermittent wavelet analysis practically applicable. This formula is expressed in the following equation:

$$a(k) = \frac{\prod_{i=-N+1}^N (\frac{1}{2} - i)}{\prod_{i=-N+1}^N (k - i)} \text{ for } k=1, \dots, N \quad (2.28)$$

C. Symlets Wavelet

Symlets are close to the corresponding wavelets suggested by Dubhesh, which is a modification of the Daubechies class. The general characteristics of the two classes are similar and are expressed in the following equation:

$$T_{so,k} = \begin{cases} (2^k)T_s & (1 \leq k \leq n) \\ (2^n) & (k = n + 1) \end{cases} \quad (2.29)$$

D. Coiflets Wavelet

And the function of standardization has $2N-1$ of the azimuth and zero also, and both functions deal with the length $6N-1$, and can be defined as this wavelet according to the following equation:

$$BW_k = \begin{cases} \frac{BW}{2^k} & (1 \leq k \leq n) \\ \frac{BW}{2^n} & (k = n + 1) \end{cases} \quad (2.30)$$

E. Biorthogonal Wavelet

This category of wavelets gives the linear pattern characteristic that is important for the reconstruction of the image, and the signal. The first wavelet is used for analysis (on the left), and the second for reconstruction (on the right) rather than one for the purpose of obtaining a useful property, and expresses this wavelet by the following equations:

$$T_{si,k+1} = 2T_{si,k} \quad 1 \leq k < n \quad (2.31)$$

$$BW_{k+1} = \frac{BW_k}{2} \quad 1 \leq k < n \quad (2.32)$$

2.12 NOISE OF IMAGE

In general, noise can be defined as undesirable information distributed in random images at the image level that scramble the image and decrease its clarity. Images are usually accompanied by various kinds of interference in image signals or signals of external influences such as signals resulting from changes in environmental conditions or in the Sensitivity of the Detector, as well as errors during transport and numbering.

2.12.1 Noise Types

The noise can be categorized mathematically into the following types:

1. Additive Noise. This noise is random and does not depend on the signal and is characterized by the following qualities:

White noise and spectral density are constant.

Additive linear The distorted image is the result of the original image (pure $R(x, y)$) with noise.

2. Multiplicative Noise.

3. Salt And Pepper Noise.

$$I(X,Y) = R(X,Y) + N(X,Y) \quad (2.33)$$

$N(x, y)$ = the non-signal-dependent noise is usually equal to zero (n).

$I(x, y)$ = distorted image (view).

$R(x, y)$ = The original image is noise-free.

c) Statistical approximations of noise distribution

There are two main types of collective noise: Gaussian distribution, uniform distribution noise and noise distribution have a close association with the physical cause of their appearance [73].

1. Multiplicative Noise

Which is a random noise based on the signal that the areas of high intensity in the picture are high noise, where the lower the intensity of the light decreased noise with them and this indicates that there is a relationship between the amount of noise and intensity of the signal and this relationship is proportionate and the statistical characteristics of this type of Noise from added noise is expressed mathematically as it comes [74][75]:

$$I(X,Y)=R(X,Y)\times F(X,Y) \quad (2.34)$$

$I(x, y)$: distorted image (viewing).

$R(x, y)$: Original noise-free image.

$F(x, y)$: random noise variable (not supported by signal and usually average).

2. Salt and pepper noise.

Salt and pepper noise differs from its predecessor because in its case some of the image points are replaced with new values, which are the noise in the form of white dots (Salt) and black (Pepper). This noise does not depend on the original values in terms of intensity and location [73],[74].

2.13 CONTRAST AND BRIGHTNESS (CB)

2.13.1 Brightness

It can be defined as the self-visual sense of light produced from a surface or from a pointless source. It is also known as an element of the sense of sight where a source seems to radiate or reflect light. That is, the brightness is the realization of a source of light. It is a measure of the reflected or scattered part of the white beam falling on the colored material [77]. The term brightness was used in optical measurement as a synonym for the term "luminance" and an error in radiometric science was used as synonym for radiological term. Therefore, the term

"brightness" should be used only to indicate the perception and sense of light. In the colour space, the brightness may be understood as the arithmetic average (μ for three coordinates, which are R, G and B). Some of three elements make the light appear brighter compared to other colors, which can be automatically modified in some show systems (M) is expressed as follows:[78]

$$\mu = \frac{R+G+B}{3} \quad (2.35)$$

μ : The arithmetic mean of the three color coordinates (R, G, B).

2.13.2 Contrast

Contrast is the ratio between object lighting and background lighting on which objects are located. The sensitivity of the contrast is dependent on the spatial distribution of the light and dark regions of image and the images can be improved using this property. The contrast feature can be used to compress and encrypt images by selecting the most frequented data and allocating them to areas most sensitive to spatial frequency [78].

2.14 OBJECTIVE QUALITY METRICS USED IN STUDY

The following measures have been applied to measure image quality

A. The Structural Similarity Index (SSIM)

Both the MSE and PSNR are the most commonly utilized standard for the full-reference image quality, but large error scores in these measurements do not always result in large structural distortions. Zhou Wang and Alan Bovik proposed the full reference to the assessment of image quality using SSIM, and based on error scores to overcome this problem in measurements. The basic SSIM algorithm in the two images requires comparison to correspond to the size correctly so that pixels can be compared with pixels. Calculations are usually carried out in a sliding window (11 x 11) with a kausset. The SSIM scale is based evaluating 3 different measurements, which are: luminance, contrast, and structure. It may be calculated as follows [66]:

$$I(x,y) = \frac{2\mu_x(x,y)\mu_y(x,y)+C1}{\mu_x^2(x,y)+\mu_y^2(x,y)+C1} \quad (2.36)$$

$$C(x,y) = \frac{2\sigma_x(x,y)\sigma_y(x,y)+C2}{\sigma_x^2(x,y)+\sigma_y^2(x,y)+C2} \quad (2.37)$$

$$S(x,y) = \frac{C3 + \sigma_{xy}(x,y)}{C3 + \sigma_x(x,y) + \sigma_y(x,y)} \quad (2.38)$$

(X and y) denote the two elements of the original and improved images, which must be identical to two different images ($\mu_x \sigma_x^2$) representing the variation and heterogeneity of the two different images in the masses (σ_{xy}):

$$\mu(x,y) = \sum_{p=-p}^p \sum_{q=-q}^q W(p,q) X(x+p, y+q) \quad (2.39)$$

$$\sigma^2(x,y) = \sum_{p=-p}^p \sum_{q=-q}^q G(p,q) [X(x+p, y+q) - \mu_x(x,y)]^2 [Y(x+p, y+q) - \mu_y(x,y)] \quad (2.40)$$

Where (p, q) G is a weighted function of kaus and is expressed by the following equation:-

$$\sum_{p=-p}^p \sum_{q=-q}^q G(p,q) = 1 \quad (2.41)$$

C1, C2 and C3 represent constants which are given according to following relationships:

$$C1 = (K1 L)^2, \quad C2 = (K2 L)^2, \quad C3 = \frac{c^2}{2} \quad (2.42)$$

(L): the dynamic rate of the sample data, ie (L = 255) contains (8 bit), $\ll 1$ k₁ and $\gg 1$ k₂ They are numerical constants. In view of the above measures, SSIM are expressed as:-

$$SSIM(x,y) = i(x,y) \cdot c(x,y) \cdot s(x,y) \quad (2.43)$$

B. Peak Signal to Noise Ratio (PSNR)

It is specified as a statistical measurement that represents the ratio between maximal possible signal power and deformation of distorted noise by compression, that is, it measures the accuracy of the image.

PSNR is measured using a logarithmic decibel in a unit called decibel and is denoted by dB as its ideal values range from 30-50 dB. The highest value of PSNR should mean that the image has better quality (Quality) and calculated from the following equation [67]:

$$PSNR = 10 * \log\left(\frac{(L-1)^2}{MSE}\right) \quad (2.44)$$

Where L is the number of grey levels and ranges from (255-0).

C. Universal Quality Index (UQI)

This standard is different from the classical measures for calculating the error rate of the image and Bovik that the model of image processing is a combination that consists of 3 factors, which

are loss of correlation, light distortion, distortion of contrast. This model is called the Universal Quality Index (UQI). This metric is defined by the following formula: [68]

$$UQI = \frac{4\bar{x}\bar{y}\sigma_{xy}}{(\bar{x}^2 + \bar{y}^2)(\sigma_x^2 + \sigma_y^2)} \quad (2.45)$$

Where the original image rate is denoted by x and y represents the processing, σ_x and σ_y is the standard deviation of original image and processing respectively, and σ_{xy} represents the variance given by the following formula [68]:

$$\sigma_{xy} = \frac{1}{N-1} \sum_{i=1}^N [(y - \bar{y})(x - \bar{x})] \quad (2.46)$$

or

$$UQI = \left(\frac{\sigma_{xy}}{\sigma_x \sigma_y} \right) \left(\frac{2\bar{x}\bar{y}}{\bar{x}^2 + \bar{y}^2} \right) \left(\frac{2\sigma_x \sigma_y}{\sigma_x^2 + \sigma_y^2} \right) \quad (2.47)$$

UQI is defined as consisting of three elements: the first is the coefficient of correlation between the original image ratio (x) and the image processing rate (y), and the image measuring the level of linear correlation between them, (1) and (1). The second element is the luminance between x and y and ranges from 0 to 1 so that the maximum is equal to 1 if they are equal. The standard deviations from those images are used as well to estimate their variance levels. Therefore, the third element in the equation is necessary to measure the similarity between the levels of contrast in images and the value between 0 and three factors: (a) the correlation coefficient, (b) the rate of similarity of light, (c) similarity on the level of contrast between them, the image quality can be assessed [68].

D. Image Fidelity (IF)

Image resolution indicates the capability of operations in reproducing images accurately with no clear distortion or loss of information. If we do not discover the difference between original image and compressed one, the conclusion that will be made is that the compression processes were visually loss-free. There is a possibility of developing computational measures of image accuracy on the basis of the human vision models due to the fact that those types of laws or judgments based on our ability of detecting the difference between images. There is a natural tendency of confusing image quality and accuracy terms, but those terms are interchangeably used but differ from each other. This standard is defined as follows [69]:

$$IF=1-\frac{\sum_{i=1}^M \sum_{j=1}^N [x(i,j)-y(i,j)]^2}{\sum_{i=1}^M \sum_{j=1}^N [x(i,j)]^2} \quad (2.48)$$

E. Root Mean Square Error (RMSE)

Referred to as square root of MSE between two original images x (i, j) and improved y (i, j). The lowest value of RMSE indicates that the image has a higher quality, Closer to the original image and calculated from the following equation [70]:

$$RMSE = \sqrt{\frac{1}{MN} \sum_{i=1}^M \sum_{j=1}^N (x(i,j)-y(i,j))^2} \quad (2.49)$$

F. Average Difference (AD)

Represen Represents rate of difference between the enhanced image and the original one. It can be defined according to the following equation [71]:

$$AD = \frac{1}{MN} \sum_{i=1}^M \sum_{j=1}^N [(x(i,j) - y(i,j))] \quad (2.50)$$

G. Correlation Quality (CQ)

$$CQ = \frac{\sum_{i=1}^M \sum_{j=1}^N x(i,j)*y(i,j)}{\sum_{i=1}^M \sum_{j=1}^N x(i,j)} \quad (2.51)$$

This measure can be represented as [72]:

X (i, j) represent the original image element of the site (i, j).

y (i, j): represent the enhanced image element in the location (i, j).

H. Visual Information Fidelity (VIFp)

It is highly important in numerous applications in image and video processing. It is therefore suggested to measure the loss of image information as a result of the process of distortion and to discover the correlation between image information and visual quality. Quality assessment systems always contribute to evaluating the visual quality of natural images and videos on

human consumption. The researchers have presented enhanced models for capturing the statistics of these natural signals. Utilizing those models, the accuracy of the information was suggested for the evaluation of the quality of the image, which relates to image quality, with the amount of data which has been shared between the original and distorted images. Therefore, this measure was proposed to measure the image information that determines the amount of information contained in the original image and also determines the amount of reference information that may be drawn from the distorted one. The vehicle of those two quantities produces a scale called the VIFP (Optical Image Accuracy Standard) to assess image quality and is defined by the following equation [85]:

$$\text{VIFp} = \frac{\sum_{j \in \text{subbands}} I(\vec{C}^{N,j}; \vec{F}^{N,j} | \vec{S}^{N,j})}{\sum_{j \in \text{subbands}} I(\vec{C}^{N,j}; \vec{E}^{N,j} | \vec{S}^{N,j})} \quad (2.52)$$

I. PSNR-HVS-M

It considered the suggested model and CSF, which is the contrast sensitivity function. For analyzing the efficiency of the presented model throughout the experiments, 155 observers sorted this group of testing images based on the order of their visual appearance and compare them with the original image that has not been distorted. The new measure, PSNRHVS-M performed better than other famous quality metrics that are reference based and showed high association with the outcomes of the subjective experiments (Kendall correlation is 0.948 and Spearman correlation is 0.984) [86]:

$$\text{PSNR}_{\text{HVSM}} = 10 \log \left(\frac{\text{MAX}^2}{\text{MSE}_H} \right) \quad (2.53)$$

J. PSNR-HVS

Those are based on the Universal Quality Index (UQI) and PSNR which is modified to consider properties of HVS. Numerous researches have confirmed that the HVS has higher sensitivity to distortions of low frequency compared to high frequency distortions. In addition to that, it is of a high sensitivity to contrast variations and noise. The participating in evaluation test of image quality [87].

$$\text{PSNR-H} = 10 \log \left(\frac{255^2}{\text{MSE}_H} \right) \quad (2.54)$$

3. PRACTICAL PART

3.1 INTRODUCTION

In this chapter; explain the database of images and videos and improve them with Matlab program.











3.2 DATABASE STUDY (VIDEOS)











The database contains the types of programs through which the videos are played. Table 3.1 shows the study database (images + videos) representing medical images and videos taken using different imaging techniques used in the study in terms of number, size and gender, will be clarified in the table 3.2 review of medical videos.

Table 3.1: The Study Database (Videos) That Represent Medical Videos

Video#	Source/ Date/ time	Video Format
1.	Hospital (Ghazi Hariri)/ 2017-11-21-13-05-03	MP4
2.	Hospital (Ghazi Hariri)/ 2017-11-21-12-42-56	FLV
3.	Hospital (Ghazi Hariri)/ 2019-9-23_13-06-07	AVI
4.	Hospital (Ghazi Hariri)/ 218-8-21_12-38-23	M4V
5.	Hospital (Ghazi Hariri)/ 2014-12-20_12-42-56	MKV
6.	Hospital (Ghazi Hariri)/ 2012-13-12_12-44-20	MOD
7.	Hospital (Ghazi Hariri)/ 2011-5-19_12-46-10	WMV
8.	Hospital (Ghazi Hariri)/ 2013-8-18_12-47-33	DVD
9.	Hospital (Ghazi Hariri)/ 2009-8-17_12-52-45	TOD
10.	Hospital (Ghazi Hariri)/ 2011-7-16_12-55-59	VOB

Table 3.2: Videos details at table 3.1.

Time and Date	sex /Age	Medical video	Medical imaging	image dilates
2017-11-21-13-05-03	Man/ 65			JPG22.4 KB (23,008 bytes)
2017-11-21-12-42-56	Woman/ 54			PNG64.9KB (66,513bytes)
2019-9-23_13-06-07	Woman/ 70			PNG 58.1KB (59,595bytes)
2018-8-21_12-38-23	Man/ 52			PNG5.3KB (77,199bytes)
2014-12-20_12-42-56	Man/ 63			PNG 62.8 KB (64,368 bytes)

2012-13-12_12-44-20	Woman/ 27			PNG49.6KB (50,815bytes)
2011-5-19_12-46-10	Man/ 57			PNG 34.KB (35,620bytes)
2013-8-18_12-47-33	Man/ 54			PNG 45.4KB (46,538bytes)
2009-8-17_12-52-45	Woman/ 67			PNG41.8KB (42,826bytes)
2011-7-16_12-55-59	Man/ 30			PNG 8.4KB (49,580bytes)

3.3 BLOCK DIAGRAM OF STUDY

The proposed block diagram of the study shown in Figure 3.1.

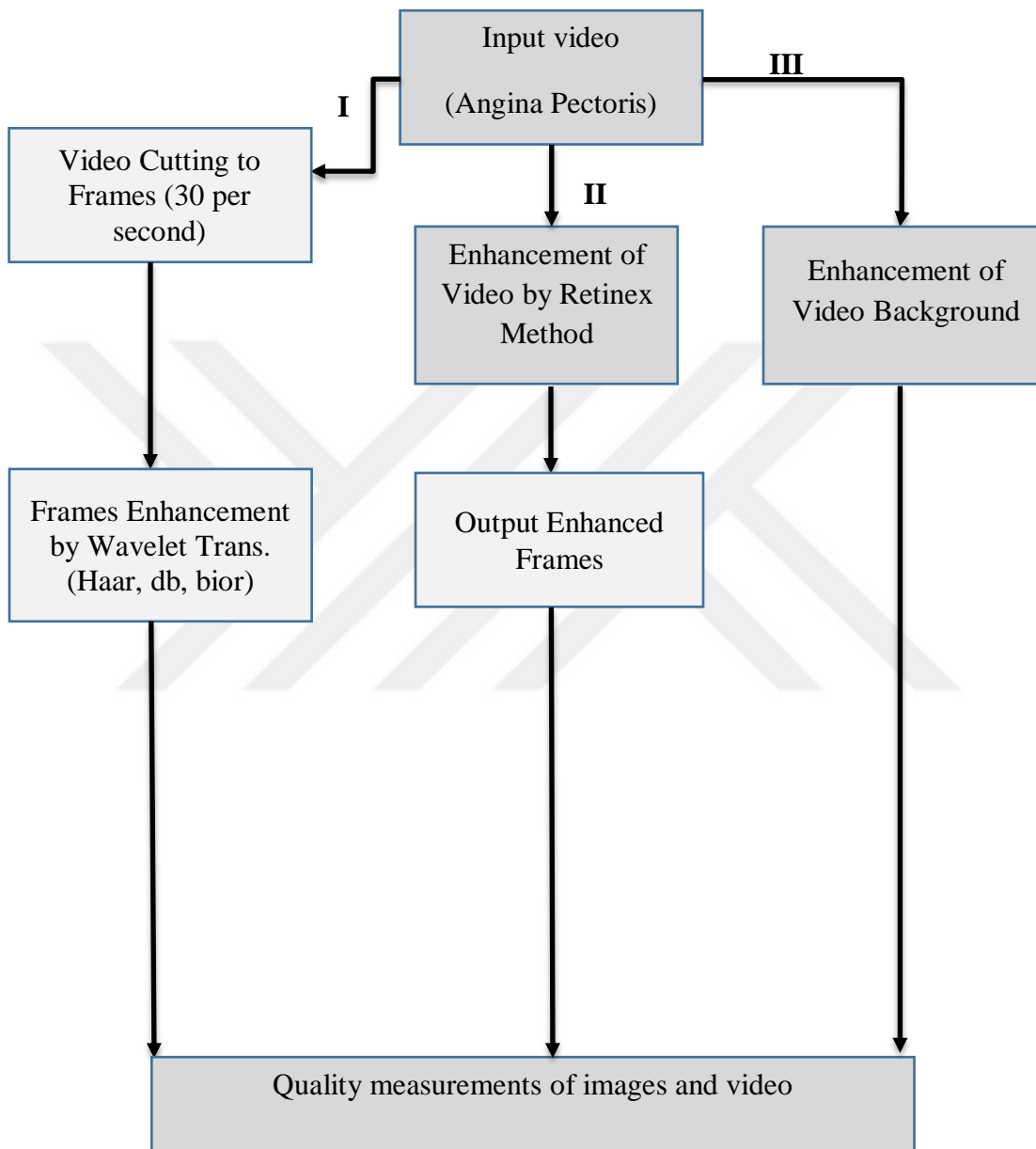


Figure 3.1: The General Diagram of present study

3.4 THE ALGORITHM OF STUDY

Figure 3.2 explains the step of extract frames from video.

Input: video
Output: Images (Frames)
Step 1: begin
Step 2: cut video to image
frames = obj. Number Of Frames
Step 3: Calculate the number of frames
Step 4: for x = 1:number of frames
Step 5: Calculate the following equation
Step 4: Sx=num2str(x);
Step 5: end
Step 6: stop

Figure 3.2: Extract Frames from Video

Figure 3.3 explains the wavelet denoising method consists of the following steps.

Input: Image
Output: denoising Image
Input: The noisy image (I) and maximum decomposition level (j)
Output:
Step1: Decompose I by the DWT for one level and obtain the wavelet coefficients
Step2: Standard deviation (σ) calculate of the noise.
Step3: Decompose by DWT for J levels and obtain the wavelet coefficients
Step4: For $j=0$ to $j-1$ do Compute I, along each direction Modify wavelet coefficients of six sub bands End
Step5: Reconstruct complex image using wavelet coefficient and corresponding scale coefficients
Step6: obtain the denoised magnitude image I from the reconstructed complex image
return The denoised magnitude image I

Figure 3.3: Wavelet denoising method

Figure 3.4 explains Retinex method.

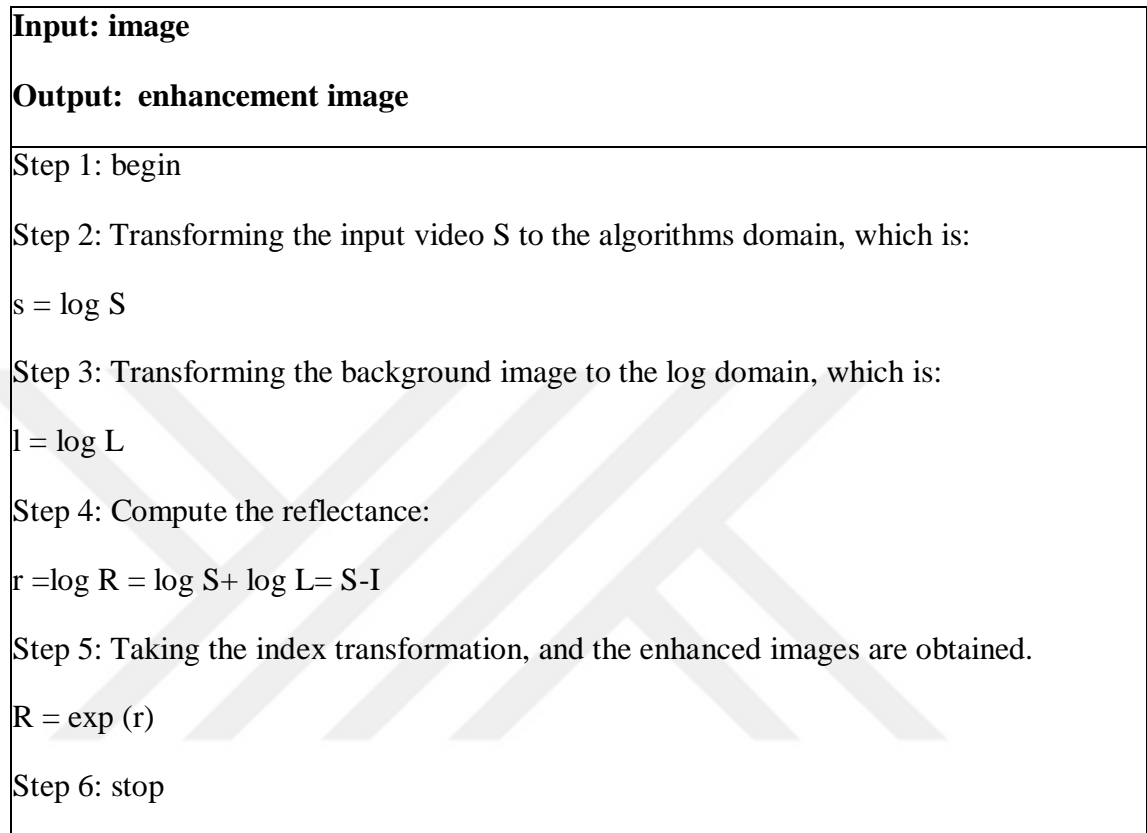


Figure 3.4: Retinex method

3.5 VIDEO CUTTING AND SPLIT

Figure 3.5 shows the program interface used to cut videos into frames, as well as, the possibility of collection and return to video.

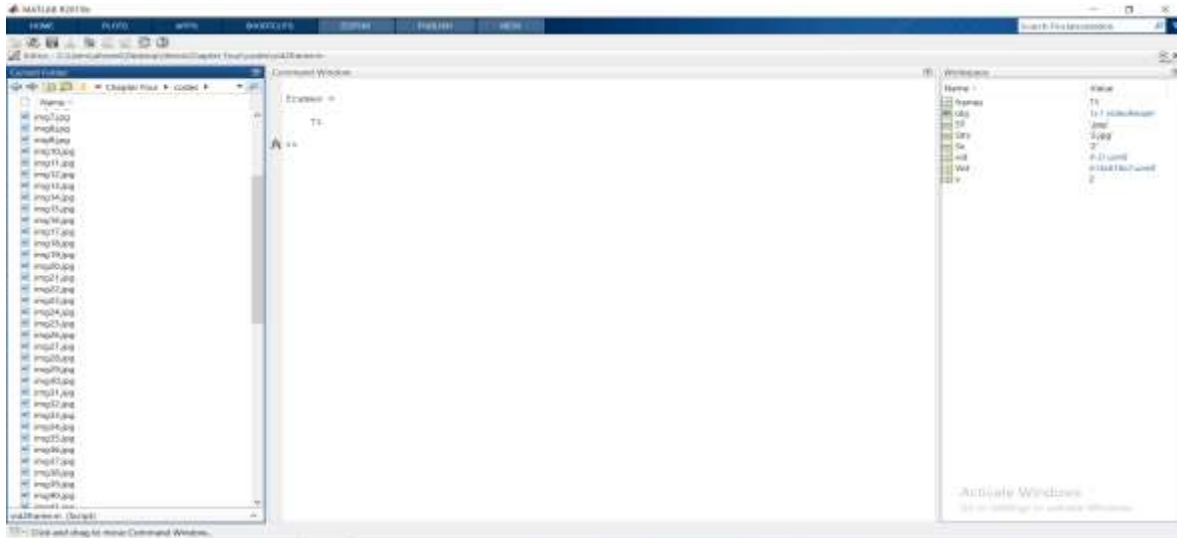


Figure 3.5: The program interface used to cut videos into frames

3.6 OPTIMIZE IMAGE USING WAVEGUIDE TECHNOLOGY

After adding Gaussian and salt and peppers to the image, the image is improved by removing this method in the ways of the waveform.

Steps to improve the image with a waveguide:

1. Access to the graphical interface of the Wavelet conversion in the program Matlab 2015a and load the image as shown in Figure 3.6.
2. Select the Wavelet conversion class (such as Haar, db, bior) and Level and press Analysis as depicted in Figure 3.7.
3. Select the resulting image from the Decomposition process at the Level selected to analyze the image data and press reconstruct to get the Approximation Image. As illustrated in Figure 3.8.

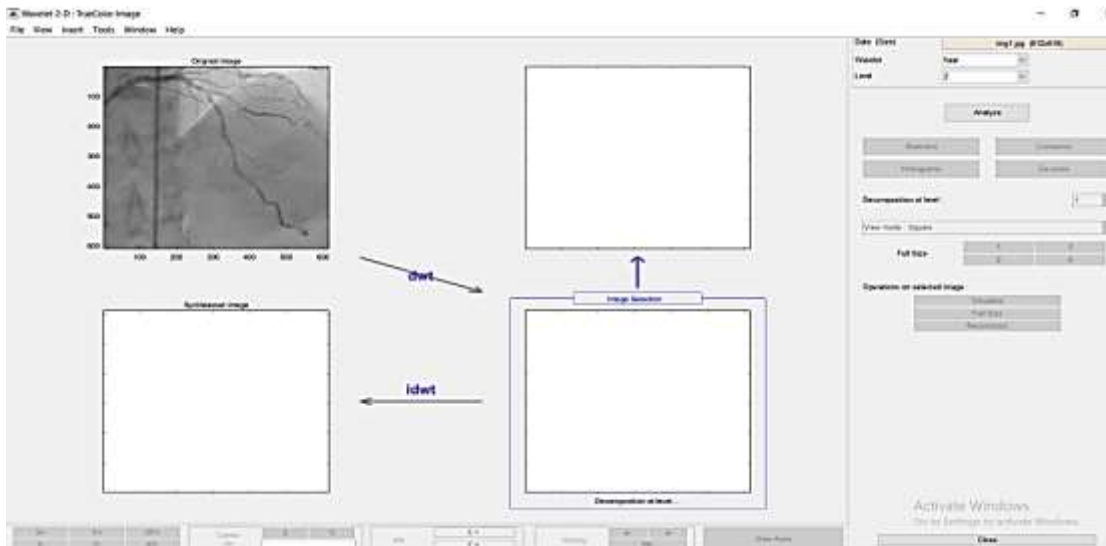


Figure 3.6: Reading the image in the Wavelet transform

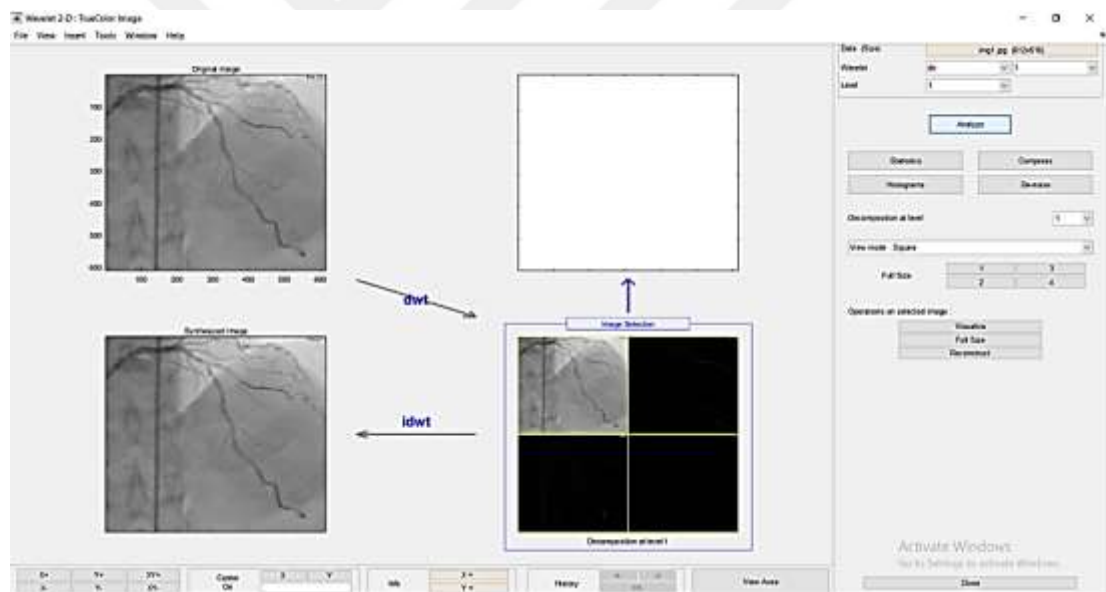


Figure 3.7: Selection of the wave and level conversion class

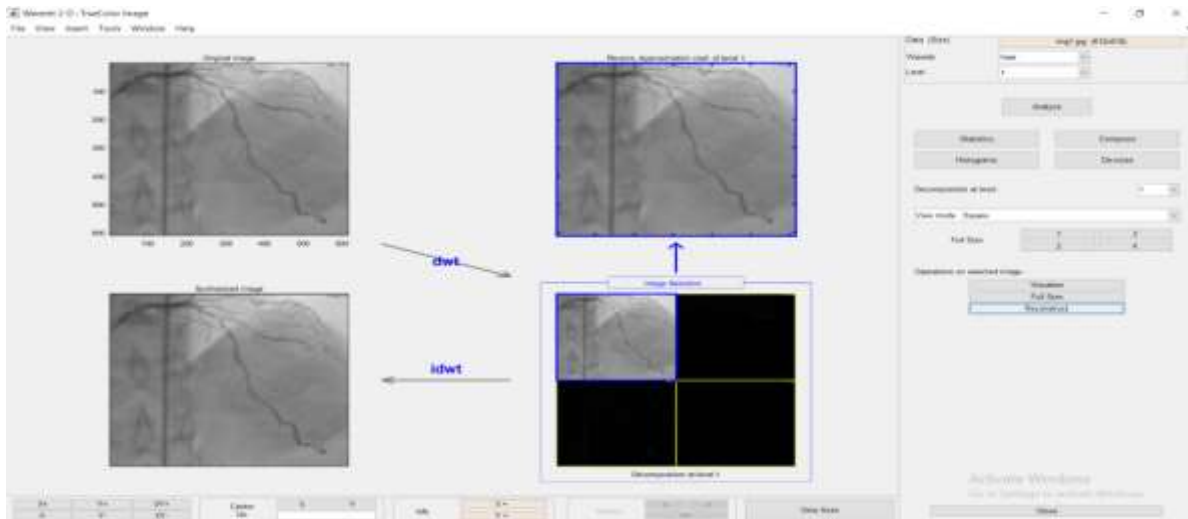


Figure 3.8: The approximate image resulting from the process of analysis and dissolution using waveguide

4. FINDINGS AND CONCLUSIONS

4.1 INTRODUCTION


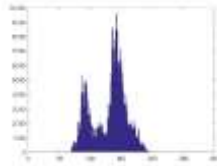

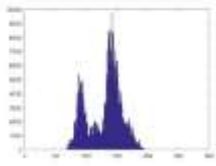

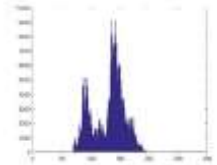

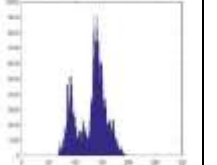
This chapter presents the results of the fourth chapter includes the presentation of the results of medical images and videos, as applied quality measures of the objective images and videos applied to medical images and videos after being improved through Wavelet Transformation and three categories (Haar, db2, bior2.2) and enhancement the Retinex method in the video. These quality measures are based on the same medical images after improving their brightness and contrast depending on the path [88].

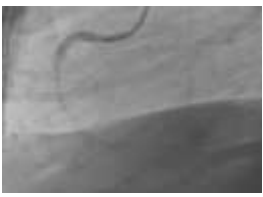
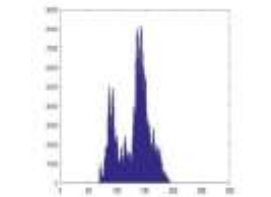

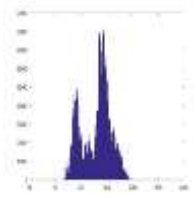

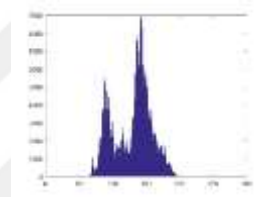

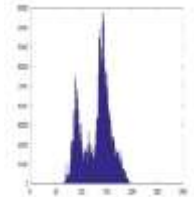

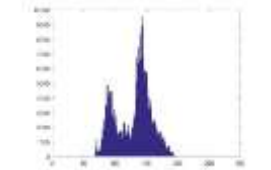

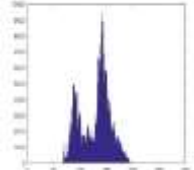
4.2 VIDEOS ENHANCEMENT


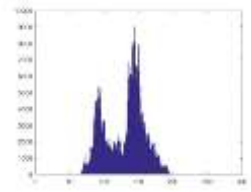

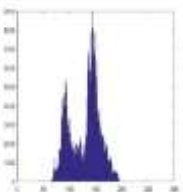

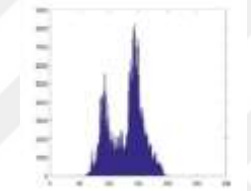

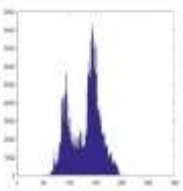

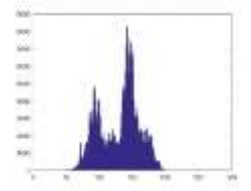

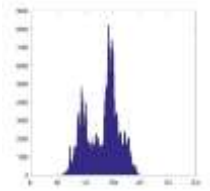
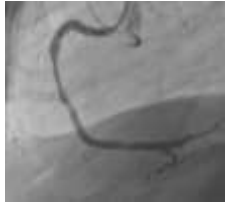
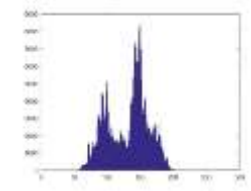

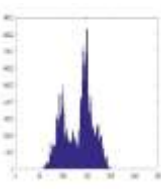
Method I): Enhancement by Wavelet Transform

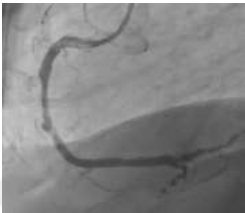
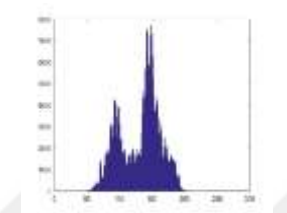

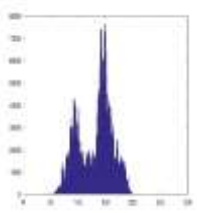

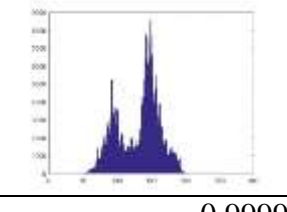

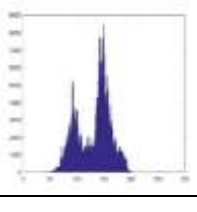

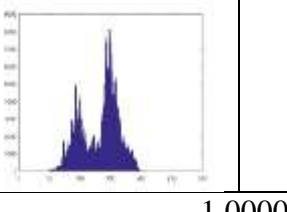

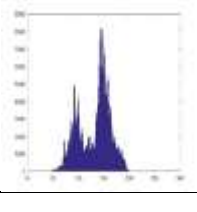
The results of quality measurements enhanced are shown table (4.1) by wavelet (Harr) method (see Appendix for db, bior).


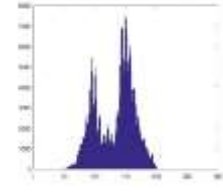
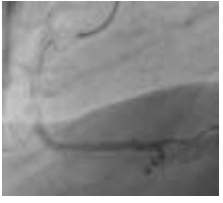
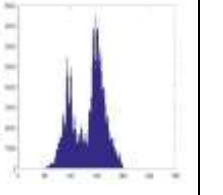
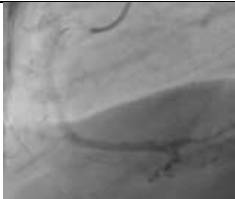
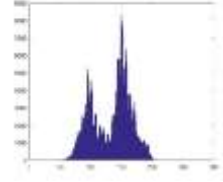
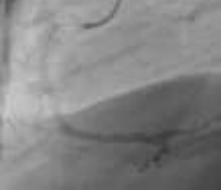
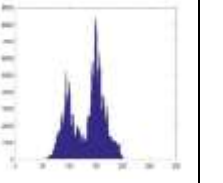

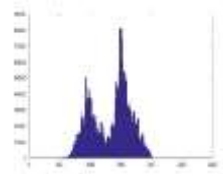

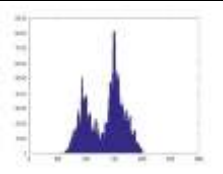
Table 4.1: The quality measurements of the image (Angina pectrios) after the application of wavelet (Haar).

Videos #	Original		Enhanced	
# 1				
IF	1			
SSIM	0.9899			
RMSE	0.4146			
PSNR	55.7772			
AD	0.0269			
CQ	135.2326			
UQI	1			
# 2				
IF	1			
SSIM	0.9904			
RMSE	42.522			
PSNR	54.7893			

AD	0.0288			
CQ	135.2483			
UQI	1			
# 3				
IF	1			
SSIM	0.9886			
RMSE	0.5094			
PSNR	53.9891			
AD	0.0374			
CQ	135.4114			
UQI	1			
# 4				
IF	1			
SSIM	0.9869			
RMSE	0.6656			
PSNR	51.6661			
AD	0.0557			
CQ	135.2399			
UQI	1			
# 5				
IF	1			
SSIM	0.985			
RMSE	0.7729			
PSNR	50.3678			
AD	0.0705			
CQ	135.0745			
UQI	1			
# 6				

				
IF	0.9999			
SSIM	0.9834			
RMSE	0.9418			
PSNR	48.6513			
AD	0.0991			
CQ	135.1107			
UQI	1			
# 7				
IF	0.9999			
SSIM	0.9833			
RMSE	0.9448			
PSNR	48.6238			
AD	0.1006			
CQ	135.186			
UQI	1			
# 8				
IF	1			
SSIM	0.9856			
RMSE	0.8114			
PSNR	49.9456			
AD	0.0839			
CQ	137.1369			
UQI	1			
# 9				


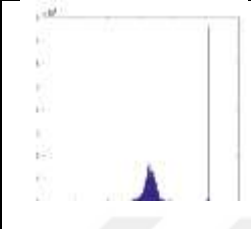
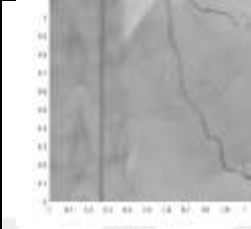
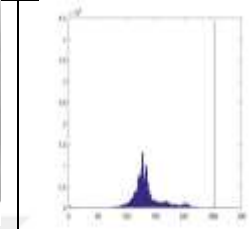

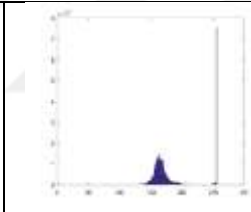
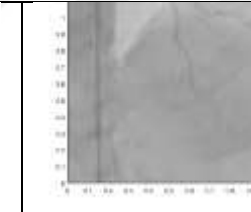
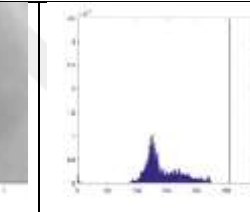

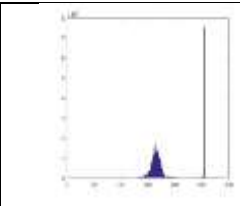

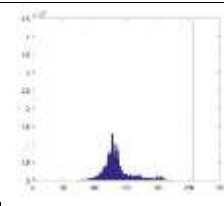
IF	1			
SSIM	0.9842			
RMSE	0.8495			
PSNR	49.5473			
AD	0.0897			
CQ	138.2878			
UQI	1			
# 10				
IF	1			
SSIM	0.9838			
RMSE	0.9123			
PSNR	48.9284			
AD	0.0977			
CQ	138.1625			
UQI	1			
# 11				
IF	0.9999			
SSIM	0.9826			
RMSE	0.9539			
PSNR	48.5407			
AD	0.1046			
CQ	138.2101			
UQI	1.0000			
# 12				
IF	1.0000			
SSIM	0.9827			
RMSE	0.9124			
PSNR	48.9271			
AD	0.0987			
CQ	138.6238			
UQI	1.0000			



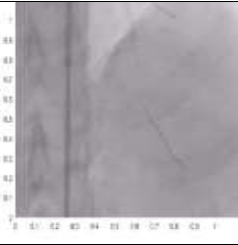
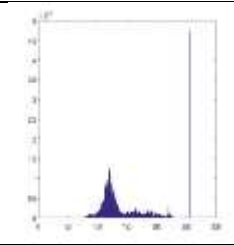

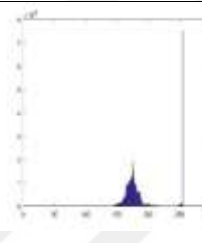
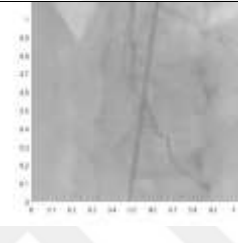
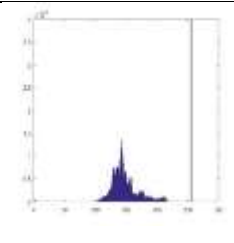

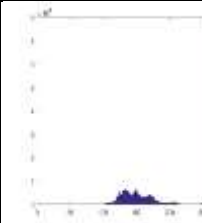
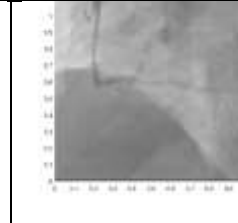
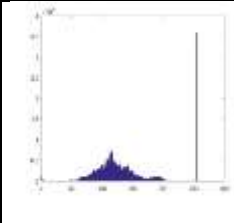
# 13				
IF	1.0000			
SSIM	0.9845			
RMSE	0.7388			
PSNR	50.7599			
AD	0.0721			
CQ	139.6442			
UQI	1.0000			
# 14				
IF	1.0000			
SSIM	0.9878			
RMSE	0.6056			
PSNR	52.4876			
AD	0.0496			
CQ	140.3425			
UQI	1.0000			
# 15				
IF	1.0000			
SSIM	0.9872			
RMSE	0.6080			
PSNR	52.4521			
AD	0.0533			
CQ	141.2909			
UQI	1.0000			


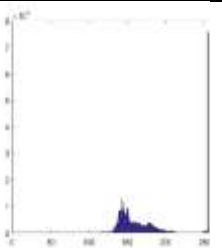

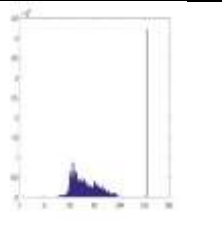
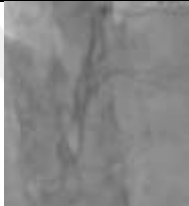
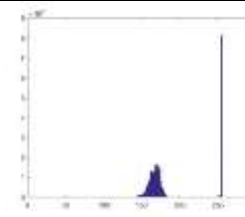

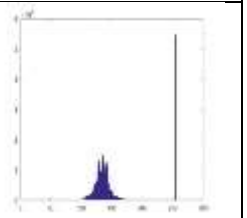

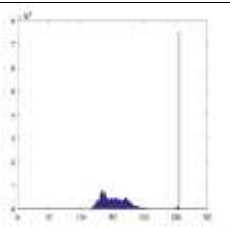

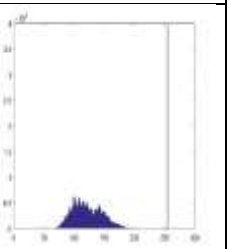

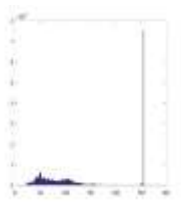
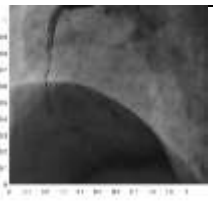
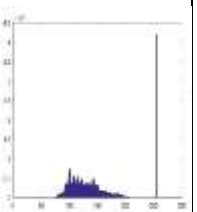
Method II): Enhancement Video by Retinex Techniques


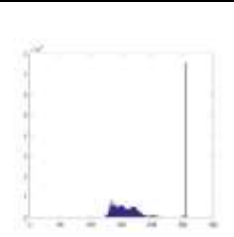

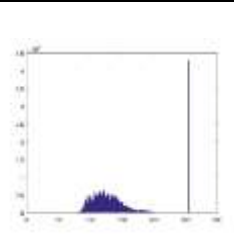

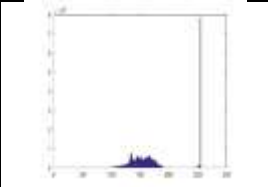

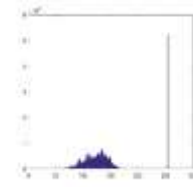

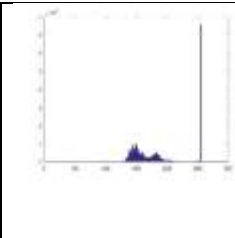
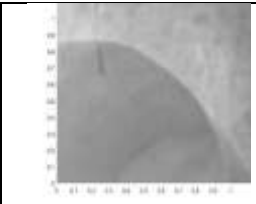
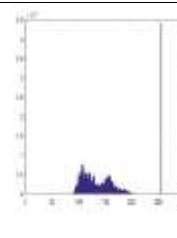
The quality measurements of video after enhancement by applied the Retinex method, as show in table (4.2).


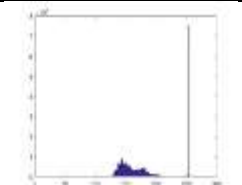

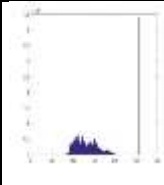

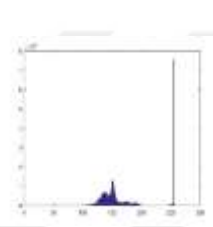

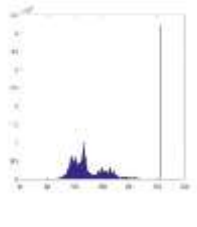
Table 4.2: The quality measurements of the image (Angina pectoris) after the application Retinex method

Videos#	Original		enhanced	
# 1				
PSNR-HVS-M	48.0822			
PSNR-HVS	47.9778			
UQI	0.8673			
PSNR	10.7275			
SSIM	0.0115			
VIF	0.0410			
# 2				
PSNR-HVS-M	48.2881			
PSNR-HVS	48.2099			
UQI	0.8794			
PSNR	10.7190			
SSIM	0.0088			
VIF	0.0387			
# 3				
PSNR-HVS-M	51.2953			
PSNR-HVS	51.1553			
UQI	0.8990			
PSNR	11.5328			
SSIM	0.0371			
VIF	0.0433			

# 4				
PSNR-HVS-M	46.7893			
PSNR-HVS	46.7501			
UQI	0.8584			
PSNR	10.5114			
SSIM	0.0196			
VIF	0.0614			
# 5				
PSNR-HVS-M	52.7092			
PSNR-HVS	52.4834			
UQI	0.9054			
PSNR	12.0905			
SSIM	0.0166			
VIF	0.0441			
# 6				
PSNR-HVS-M	45.9285			
PSNR-HVS	45.8769			
UQI	0.8142			
PSNR	9.8878			
SSIM	0.0117			
VIF	0.0439			

# 7				
PSNR-HVS-M	47.1205			
PSNR-HVS	47.0594			
UQI	0.8602			
PSNR	10.8843			
SSIM	0.0125			
VIF	0.0378			
# 8				
PSNR-HVS-M	50.2663			
PSNR-HVS	50.1091			
UQI	0.8895			
PSNR	11.6457			
SSIM	0.0286			
VIF	0.0555			
# 9				
PSNR-HVS-M	46.4672			
PSNR-HVS	46.4123			
UQI	0.8329			
PSNR	10.2777			
SSIM	0.0083			
VIF	0.0425			
# 10				

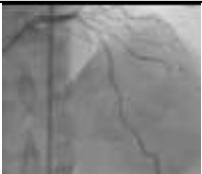
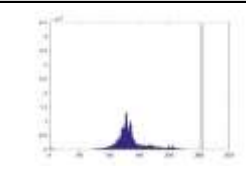

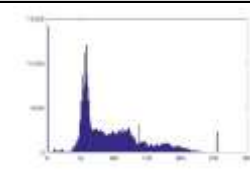
PSNR-HVS-M	47.5093			
PSNR-HVS	47.4479			
UQI	0.6675			
PSNR	8.5739			
SSIM	0.0173			
VIF	0.0617			
# 11				
PSNR-HVS-M	46.8491			
PSNR-HVS	46.7914			
UQI	0.8498			
PSNR	10.5649			
SSIM	0.0139			
VIF	0.0518			
# 12				
PSNR-HVS-M	47.2699			
PSNR-HVS	47.1871			
UQI	0.8439			
PSNR	10.0749			
SSIM	0.0176			
VIF	0.0528			
# 13				
PSNR-HVS-M	47.4433			
PSNR-HVS	47.4019			
UQI	0.8571			
PSNR	10.7344			
SSIM	0.0107			
VIF	0.0474			


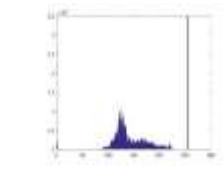
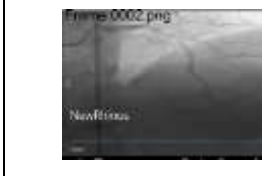
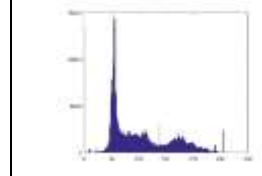

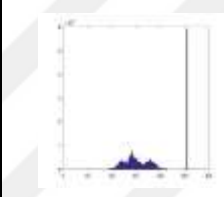

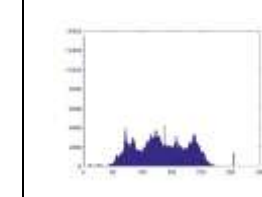

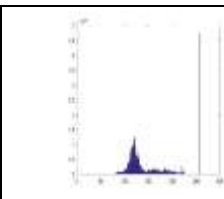
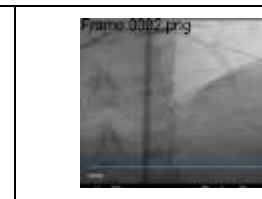
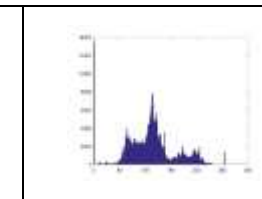
# 14				
PSNR-HVS-M	47.3581			
PSNR-HVS	47.3089			
UQI	0.8572			
PSNR	10.7292			
SSIM	0.0104			
VIF	0.0404			
# 15				
PSNR-HVS-M	46.2068			
PSNR-HVS	46.1699			
UQI	0.8279			
PSNR	10.1799			
SSIM	0.0013			
VIF	0.0518			


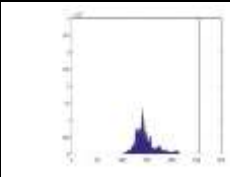

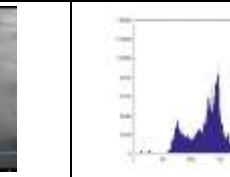

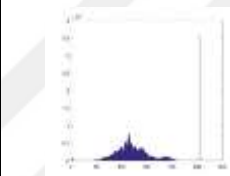

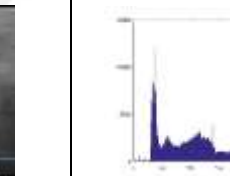

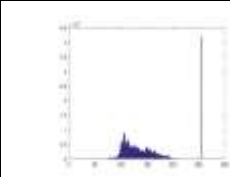

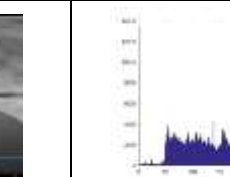

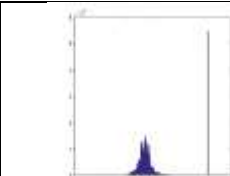
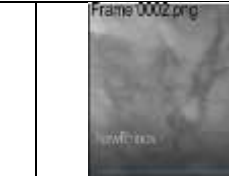
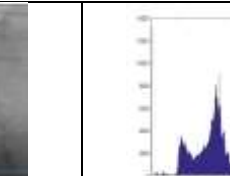
Method III): Video Background Enhancement (Extract Movie Frame)

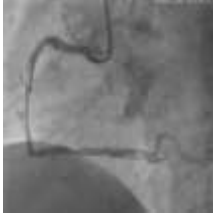
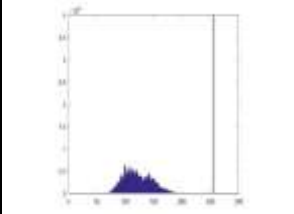
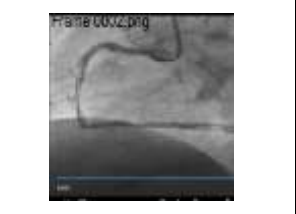
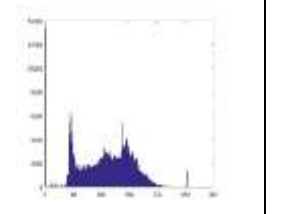
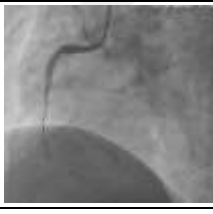
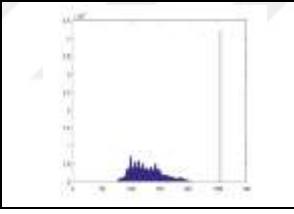

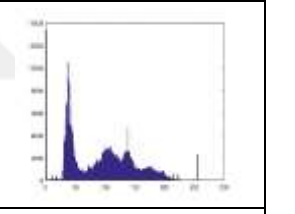

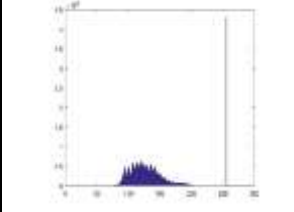

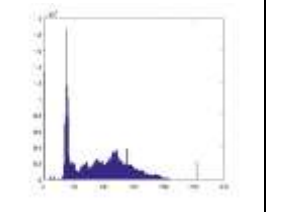
The results of quality measurements of video enhanced are shown table (4.3) after Video Background Enhancement.

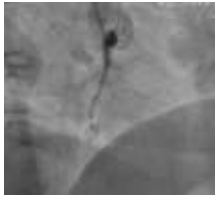
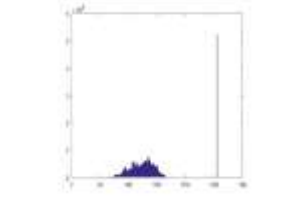

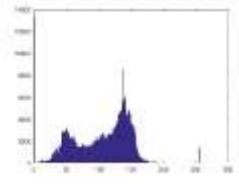

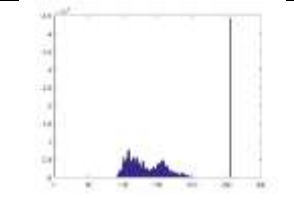
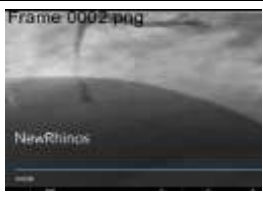
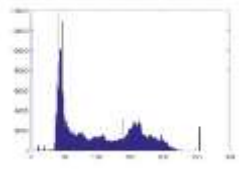

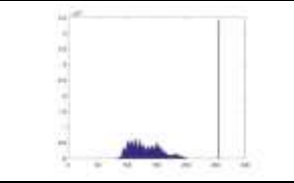

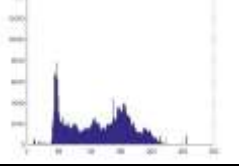
TABLE 4.3: the quality measurements of the video background (extract movie frame) enhancement


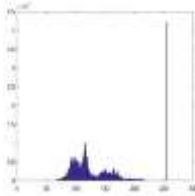

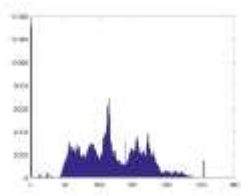
Videos #	Original video		Enhanced video	
# 1				
PSNR-HVS-M	47.4692			
PSNR-HVS	47.3479			
UQI	0.7220			
PSNR	10.0988			

SSIM	0.0089			
VIF	0.0625			
# 2				
PSNR-HVSM	48.2147			
PSNR-HVS	48.115			
UQI	0.7266			
PSNR	10.5097			
SSIM	0.0209			
VIF	0.0929			
# 3				
PSNR-HVS-M	47.922			
PSNR-HVS	47.7959			
UQI	0.8507			
PSNR	11.5263			
SSIM	0.0115			
VIF	0.0614			
# 4				
PSNR-HVSM	50.3341			
PSNR-HVS	50.2066			
UQI	0.8506			
PSNR	12.0326			
SSIM	0.0017			
VIF	0.0772			

# 5				
PSNR-HVS-M	47.7609			
PSNR-HVS	47.6262			
UQI	0.8729			
PSNR	12.2483			
SSIM	0.0052			
VIF	0.0587			
# 6				
PSNR-HVS-M	48.2024			
PSNR-HVS	48.0873			
UQI	0.6905			
PSNR	10.1071			
SSIM	0.0081			
VIF	0.0576			
# 7				
PSNR-HVS-M	47.9905			
PSNR-HVS	47.8685			
UQI	0.8270			
PSNR	11.3080			
SSIM	0.0175			
VIF	0.0676			
# 8				
PSNR-	46.4865			

HVSM				
PSNR-HVS	46.3633			
UQI	0.8258			
PSNR	11.1302			
SSIM	0.0019			
VIF	0.0770			
# 9				
PSNR-HVSM	47.7526			
PSNR-HVS	47.6437			
UQI	0.7962			
PSNR	11.3232			
SSIM	0.0172			
VIF	0.0779			
# 10				
PSNR-HVSM	47.424			
PSNR-HVS	47.3327			
UQI	0.6844			
PSNR	9.6469			
SSIM	0.0026			
VIF	0.0684			
# 11				
PSNR-HVSM	47.4257			
PSNR-HVS	47.326			
UQI	0.6940			
PSNR	9.7802			

SSIM	-0.0052			
VIF	0.0567			
# 12				
PSNR-HVSM	48.1206			
PSNR-HVS	47.9705			
UQI	0.8007			
PSNR	11.2186			
SSIM	0.0027			
VIF	0.0731			
# 13				
PSNR-HVSM	47.9266			
PSNR-HVS	47.8419			
UQI	0.6914			
PSNR	9.7602			
SSIM	0.0075			
VIF	0.0676			
# 14				
PSNR-HVSM	47.9908			
PSNR-HVS	47.881			
UQI	0.7803			
PSNR	10.8587			
SSIM	0.0139			
VIF	0.0725			

# 15				
PSNR-HVSM	48.2041			
PSNR-HVS	48.1342			
UQI	0.8125			
PSNR	10.6592			
SSIM	0.0118			
VIF	0.0651			

4.3 DISCUSSION AND CONCLUSIONS

1. Enhancement of medical images and videos has a significant impact on medical treatment and diagnosis.
2. The angina pectoris is very important in determining which artery to operate (important areas).
3. Wavelet transform has an important role in the initial rendering of images, in terms of highlighting the most important details of images, removing (or reducing) noise.
4. The Retinex method showed the best results for the enhancement of images through quality coefficients.
5. The angina pectoris can be directly enhancement within a short period of time.

4.4 FUTURE WORKS

1. Edge enhancement of medical images and videos.
2. Use the PAC method to improve angina pectoris.

REFERENCES

- [1] Rioul, O. and Pierre, Duhamel, "Fast algorithms for discrete and continuous wavelet transform", Institute of Electrical and Electronics Engineers (IEEE) Trans, 1992.
- [2] R. C. Gouzaliz, R. E. Wood, "Digital image processing", Addison Wesley 1992.
- [3] R. C. Gouzalez, R. E. Woods., S. L. Eddins, "Digital image processing using Matlab". Parson Prentice-Hall, 2004.
- [4] I. T. Young. J. Gerbrands and L. J. Van Vliet, "Fundamental of Image processing" printed in Netherlands at the Delft Univ. of Technology, 1998.
- [5] Thompson, Paul M., et al. Genetic influences on brain structure. Nature neuroscience, 2001.
- [6] Young, Ian T.; Gerbrands, Jan J.; Van Vliet, Lucas J. Fundamentals of image processing. Delft: Delft University of Technology, 1998.
- [7] John.R.Jenson , " Introductory Digital Image Processing A Remote Sensing Perspective", Prentice –Hall,1886.
- [8] Lain J. and David. "Coding wavelet coefficients of images", International Conference on DSP proceeding, pp. 37-40,1996.
- [9] Sonja Grgic, Mislav Grgic, Member, IEE, and Branka Zovko-Cihlar, "Performance Analysis of Image Compression Using Wavelets", vol. Transactions on industrial electronics 48, 3, 2001.
- [10] Damon M. Chandler, Member, IEEE, and Sheila S. Hemami, Senior, "VSNR: A Wavelet-Based Visual Signal-to-Noise Ratio for Natural Images", vol. 16, 9, 2007.
- [11] N. Ponomarenko, V. Lukin, A. Zelensky, K. Egiazarian, M. Carli, F. Battisti, "TID2008 - A Database for Evaluation of Full-Reference Visual Quality Assessment Metrics", Advances of Modern Radioelectronics, vol. 10, pp. 30-45, 2009.
- [12] Alnazer Hamza, M J Alport and W I Rae, "Automatic Scoring of American College of Radiology (ACR) Phantom Image Using Image Processing Technique",vol. 10(2) 2009.
- [13] Lin Zhanga, Lei Zhanga1, and Xuanqin Moub, "RFSIM: A Feature Based Image Quality Assessment Metric Using Riesz Transforms", 26-29, 2010.
- [14] Venkateshwarlu, K., and Anju Guide Bala. Image enhancement using fuzzy inference system. Diss. 2010.

- [15] Bankman, Isaac. Handbook of medical image processing and analysis. Elsevier, 2008.
- [16] Lehmann, Thomas Martin; Gonner, Claudia; Spitzer, Klaus. Survey: Interpolation methods in medical image processing. IEEE transactions on medical imaging, 1999.
- [17] Grossman, William. Grossman's cardiac catheterization, angiography, and intervention. Lippincott Williams & Wilkins, 2006.
- [18] Lin Zhang, Student Member, IEEE, Lei Zhang, Member, IEEE, Xuanqin Mou, Member, IEEE, and David Zhang, Fellow, IEEE, "FSIM: A Feature Similarity Index for Image Quality Assessment", vol. 20, 8, 2011.
- [19] Ravi et al., International Journal of Advanced Research in Computer Science and Software Engineering 2 (11), 2012.
- [20] Kanwaljot S. S., Baljeet S. K., Ishpreet S. V., "Medical Image Denoising In The Wavelet Doma in Using Haar And DB3 Filtering", Department of CSE and IT, BBSBEC/PTU, Punjab, India, (Print) 2319-1821, vol. 1, Issue 1, pp. 01-08, 2012.
- [21] Von ramm, Olaf T.; Smith, Stephen W.; Pavy, Henry G. High-speed ultrasound volumetric imaging system. II. Parallel processing and image display. IEEE transactions on ultrasonics, ferroelectrics, and frequency control, 1991.
- [22] Rafael C. Gonzalez and Richard, E. Woods "Digital Image Processing". Third Edition-2009.
- [23] Aboul Ella Hassanien, Amr Badr, "A Comparative Study on Digital Mamography Enhancement Algorithms Based on Fuzzy Theory" Studies in Informatics and Control, vol. 12, 1, 2003.
- [24] Tamalika Chaira, Ajoy kumar Raj, "Fuzzy image Processing and Applications with MATLAB" CRC Press 2010.
- [25] Yawalkar, Pallavi H., and PN Pusdekar. "A Review on low light video enhancement using image processing technique." International Journal of Advanced Research in Computer and Communication Engineering 4.1, 2015.
- [26] Henrik Malm Magnus Oskarsson Eric Warrant "Adaptive enhancement and noise reduction in very low light-level video" IEEE 11th International Conference on Computer Vision, 2007.
- [27] Qing Xu^{1, 2}, Hailin Jiang¹, Riccardo Scopigno³, and Mateu Sbert⁴ "A New Approach For Very Dark Video Denoising And Enhancement", Proceedings of 2010 IEEE 17th International Conference on Image Processing, 26-29, 2010.

- [28] Jinhui Hu, Ruimin Hu, zhongyuan Wang, Yang Gong, Mang Duan, “Kinect depth based Enhancement for low light surveillance image” IEEE International Conference on Image Processing, 2013.
- [29] F. Durand and J. Dorsey, Fast bilateral filtering for the display of high dynamic range images, Proc. of the 29th International Conference and Exhibition on Computer Graphics and Interactive Techniques, pp. 257-266, 2002.
- [30] E. Reinhard, G. Ward, S. Pattanaik and P. Debevec, High dynamic range imaging: acquisition, display, and image-based lighting, Morgan Kaufmann Publishers Incorporated, San Francisco, CA, 2005.
- [31] T. O. Aydin, R. Mantiuk, K. Myszkowski and H. P. Seidel, Dynamic range independent image quality assessment, Proc. of the 35th International Conference and Exhibition on Computer Graphics and Interactive Techniques, pp. 1-10, 2008.
- [32] Y. S. Heo, K. M. Lee, S. U. Lee, Y. SMOon and J. Y. Cha, Ghost-free high dynamic range imaging, Proc. of Asian Conference on Computer Visio, Lecture Notes in Computer Science, pp. 486-500, 2011.
- [33] P. E. Debevec, Rendering synthetic objects into real scenes: bridging traditional and image-based graphics with global illumination and high dynamic range photography, Proc. of the 25th Annual Conference on Computer Graphics and Interactive Techniques, pp. 189-198, 2008.
- [34] W. Zhang and W. K. Cham, Gradient-direct composition of multi-exposure images, Proc. of the IEEE Conference on Computer Vision and Pattern Recognition, pp. 530-536, 2010.
- [35] P. Didyk, R. Mantiuk, M. Hein and H. P. Seidel, Enhancement of bright video features for HDR displays, Computer Graphics Forum, vol. 27, no. 4, pp. 1265-1274, 2008.
- [36] Morel, Jean Michel; Petro, Ana Belén; Sbert, Catalina. A PDE formalization of Retinex theory. IEEE Transactions on Image Processing, 2010.
- [37] D.J. Jobson, Z.U. Rahman, and G.A. Woodell, “Properties and performance of a center/surround retinex,” IEEE Trans. on Image Processing, vol. 6, no. 3, pp. 451– 462, 1996.
- [38] Osman Nuri Ucan; ÖĞÜŞLÜ, Ender. A non-linear technique for the enhancement of extremely non-uniform lighting images. Journal of Aeronautics and Space Technologies, 2007.

- [39] Rahman Ziaur, Jobson D J, Woodell G A. Retinex processing for automatic image enhancement [J]. Journal of Electronic Imaging, 2004.
- [40] E. Land and J. McCann, "Lightness and retinex theory," J. Opt. Soc. Amer., vol. 61, no. 1, pp. 1–11, 1971.
- [41] E. H. Land, "The retinex theory of color vision," Scientific American, vol. 237, no. 6, pp. 108–128, 1977.
- [42] Mrs. Anjali Chandra, Bibhudendra Acharya, Mohammad Imroze Khan "RETINEX IMAGE PROCESSING: IMPROVING THE VISUAL REALISM OF COLOR IMAGES" International Journal of Information Technology and Knowledge Management, July-December 2011.
- [43] G. D. Finlayson, Color Constancy in Diagonal Chromaticity Space, In Proceedings: Fifth International Conference on Computer Vision, pp 218-223, IEEE Computer Society Press, 1995.
- [44] D. J. Jobson, Z. Rahman, and G. A. Woodell, —Retinex Image Processing: Improved Fidelity To Direct Visual Observation, Proceedings of the IS&T/SID Fourth Color Imaging Conference: Color Science, Systems and Applications, Scottsdale, Arizona, November, pp. 124-126, 1996.
- [45] X. Dong, Y. Pang, and J. Wen, "Fast efficient algorithm for enhancement of low lighting video," in Proc. IEEE Conf. on Multimedia and Expo, July 2011.
- [46] D.J. Jobson, Z. Rahman, G.A. Woodwell, A multiscale Retinex for bridging the gap between color images and the human observation of scenes, IEEE Trans. Image Process. 6(1997).
- [47] Y. K. Park, S.L. Park, J.K. Kim, Retinex method based on adaptive smoothing for illumination invariant face recognition, Signal Process. 88(2008).
- [48] Siddesha, K.; Naryan, Kavitha. Frequency domain based msrccr method for color image enhancement. International Journal of Research in Engineering and Advanced Technology, 2014.
- [49] Glenn A. Woodell, Daniel J. Jobson and Zia-ur Rahman, "United States Patent", Patent No: US 6,834,125 B2, Dec. 21, 2004.
- [50] Z. Rahman, G. A. Woodell, and D. J. Jobson, "A Comparison of the Multiscale Retinex With Other Image Enhancement Techniques," Proceedings of the IS&T 50th Anniversary Conference, May 1997.
- [51] Land, Edwin H.; McCann, John J. Lightness and retinex theory. Josa, 61.1: 1-11, 1971.


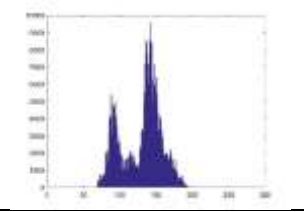

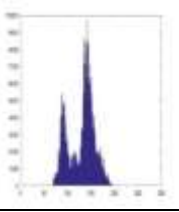

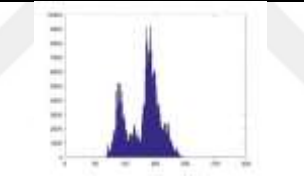

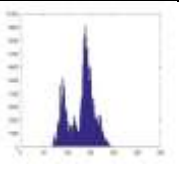

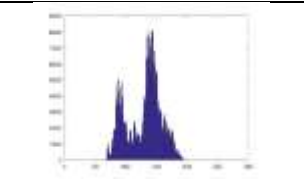

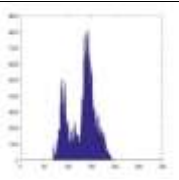
- [52] Mccann, John J. Capturing a black cat in shade: past and present of Retinex color appearance models. *Journal of Electronic Imaging*, 13.1: 36-48, 2004.
- [53] Land, Edwin H. An alternative technique for the computation of the designator in the retinex theory of color vision. *Proceedings of the national academy of sciences*, 83.10: 3078-3080,1986.
- [54] Mccann, John. Lessons learned from mondrians applied to real images and color gamuts. In: *Color and imaging conference*. Society for Imaging Science and Technology, p. 1-8,1999.
- [55] GORGEL, Pelin; SERTBAS, Ahmet; Osman Nuri Ucan. A wavelet-based mammographic image denoising and enhancement with homomorphic filtering. *Journal of medical systems*, 2010.
- [56] CEYLAN, Murat, Osman Nuri Ucan, et al. A novel method for lung segmentation on chest CT images: complex-valued artificial neural network with complex wavelet transform. *Turkish Journal of Electrical Engineering & Computer Sciences*, 2010.
- [57] Graps, A. "An Introduction to wavelet.IEEE", *Computer Society* vol. 2, No. 2, pp. 50-61, 1995.
- [58] Ibrahim. I. Auraiby, "image enhancement using wavelet transform", Thesis, Military Engineering College, 2001.
- [59] Quba, Abdul-Rahman. "Multispectral image fusion using wavelet transform", M. Sc. Thesis, Computer Science Dept., College of Science, University of Mosul, 82 P, 2001.
- [60] Sadiq H. L., "Compression and enhancement of digital image with wavelet transform", Thesis, Babylon University, 2001.
- [61] GORGEL, Pelin, Osman Nuri Ucan, et al. Mammographic mass classification using wavelet based support vector machine. *Istanbul University-Journal of Electrical & Electronics Engineering*, 2009, 9.1: 867-875.
- [62] GÖRGEL, Pelin; SERTBAS, Ahmet; Osman Nuri Ucan. Computer-aided classification of breast masses in mammogram images based on spherical wavelet transform and support vector machines. *Expert Systems*, 2015, 32.1: 155-164.
- [63] Hubbard, B. B., "The world according to wavelets", *The story of a Mathematical Technique In The Making*. AK Peters Ltd. Wellesley, MA., 1996.
- [64] Cheung, H. and Schrack, G., "Progressive image transmission by linear quadtree coding and wavelet transform", *13th International Conference on DSP Proceeding*, pp. 475-478, 1997.


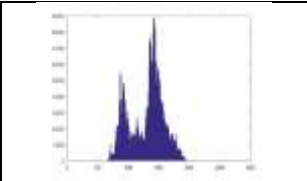
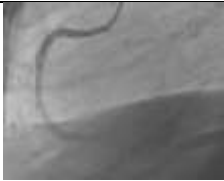
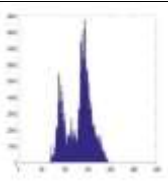

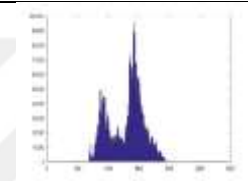
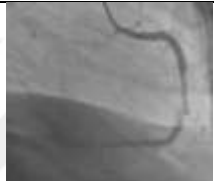
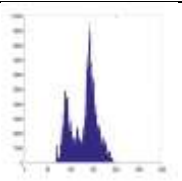

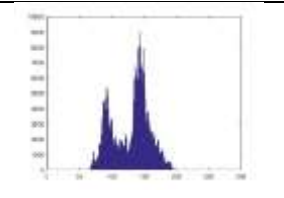

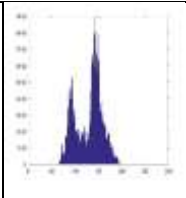

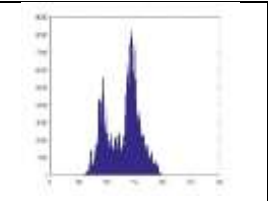

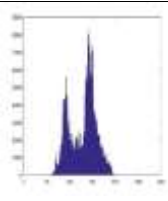
- [65] Kristan Sndenbergl "the haar wavelet transform", University of Colorado, 2000.
- [66] Wang Zhou, Bovik, Alan C., Sheikh, Hamid R., and Simoncelli, Eero P. Image Quality Assessment: From Error Visibility to Structural Similarity. IEEE Transactions on Image Processing, vol.13, Issue 4, pp. 600–612,2004.
- [67] H.R. Sheikh, M.F. Sabir, and A.C. Bovik, "A statistical evaluation of recent full reference image quality assessment algorithms", IEEE Trans. on Image Processing, vol. 15, no. 11, pp. 3440-3451, 2006.
- [68] Zhou Wang and Alan C. Bovik, "A Universal Image Quality Index," IEEE Signal Processing Letters, vol. 9, no. 3, pp. 81-84, Mar. 2002.
- [69] S. J. Daly, "The visible difference predictor: an algorithm for the assessment of image fidelity," SPIE: Human Vision, Visual Processing, and Digital Display 111, Ed Rogowitz, Allebach and Klein, 1666, pp. 2-15, 1992.
- [70] Gonzalez and Woods, "Digital Image Processing using MATLAB", Prentice Hall, New Delhi, India, 2006.
- [71] M. N.Nobi and M.A. Yusuf, "A new method to remove noise in magnetic resonance and ultrasound images," J.Sci.Res.3 (1), pp.81-89, 2011.
- [72] Wang, Yubing. Survey of objective video quality measurements. 2006.
- [73] Huda Shawki Khilil AL-Ghrabi, "Quantum analysis of noise in Photonic system", M.Sc. Thesis, physics Dept, College of Education for Woman, Baghdad University, (2001).
- [74] Al-Lihebi, A.A., "Linear digital restoration Filter", M.Sc. Thesis, Baghdad University. Collogr of Education for women, (1998).
- [75] "Brightness" in Federal Standard 1037C, the Federal Glossary of Telecommunication Terms (1996).
- [76] Gonzalez, R.C. and Wintz, P, "Digital image processing", Addison-wistely, 1987.
- [77] B. G. Haskell and A. Puri, MPEG Video Compression Basics,2011.
- [78] M. A. T. Figueiredo, J. M. N. Leit~ao, and A. K. Jain. On Fitting Mixture Models. In Emmcvpr, pp. 54–69, 1999.
- [79] P. Yap and P. Raveendran. Image focus measure based on Chebyshev moments. In Vision, Image and Signal Processing, IEE Proceedings, volume 151, pp. 128–136, 2004.
- [80] X. Li. Blind Image Quality Assessment. In Image Processing. 2002.International Conference on, pp. 449–452. IEEE, 2002.


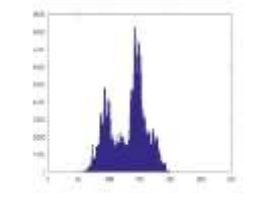

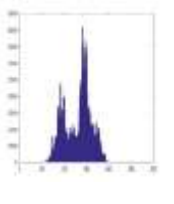

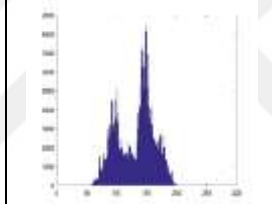

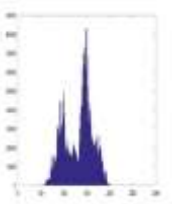

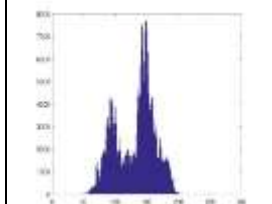

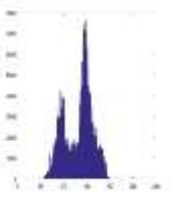
- [81] Gharbi, Hana; Bahroun, Sahbi; Zagrouba, Ezzeddine. A Novel Key Frame Extraction Approach for Video Summarization. In: Visigrapp (3: VISAPP). 2016.
- [82] JIN, Meiguang; Meishvill, Givi; Favaro, Paolo. Learning to extract a video sequence from a single motion-blurred image. In: Proceedings of the IEEE Conference on Computer Vision and Pattern Recognition. 2018.
- [83] Z. Wang, H. R. Sheikh, and A. C. Bovik, "Objective video quality assessment," In The Handbook of Video Databases: Design and Applications, B. Furht and O. Marques, Eds. Boca Raton, FL: CRC Press, 2003.
- [84] Ponomarenko, Nikolay, et al. On between-coefficient contrast masking of DCT basis functions. In: Proceedings of the third international workshop on video processing and quality metrics, 2007.
- [85] Egiazarian, Karen, et al. New full-reference quality metrics based on HVS. In: Proceedings of the Second International Workshop on Video Processing and Quality Metrics. 2006.
- [86] Ponomarenko N, Silvestri F, Egiazarian K, Carli M, Astola J, Lukin V. On between-coefficient contrast masking of DCT basis functions. In Proceedings of the third international workshop on video processing and quality metrics 2007.
- [87] Egiazarian K, Astola J, Ponomarenko N, Lukin V, Battisti F, Carli M. New full-reference quality metrics based on HVS. In Proceedings of the Second International Workshop on Video Processing and Quality Metrics 2006.
- [88] Ahmed R. Ibrahim, Osman Nuri Ucan, Ziad M. Abood, Oguz Bayat. Assessment the Quality of Medical Videos (Angina Pectoris) Enhancement. Submitted to AURUM Journal of Engineering Systems and Architecture, 2019.

APPENDIX A


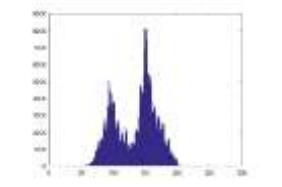

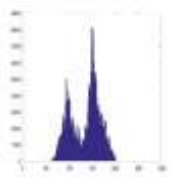
THE QUALITY MEASUREMENTS OF THE IMAGE (ANGINA PECTORIS) AFTER THE APPLICATION OF WAVELET (DB2)

Videos #	Original		Enhanced	
# 1				
IF	1			
SSIM	0.9899			
RMSE	0.4146			
PSNR	55.7772			
AD	0.0269			
CQ	135.2326			
UQI	1			
# 2				
IF	1			
SSIM	0.9904			
RMSE	0.4646			
PSNR	54.7893			
AD	0.0288			
CQ	135.2483			
UQI	1			
# 3				
IF	1			
SSIM	0.9886			
RMSE	0.5094			
PSNR	53.9891			
AD	0.0374			
CQ	135.4114			
UQI	1			

# 4				
IF	1			
SSIM	0.9869			
RMSE	0.6656			
PSNR	51.6661			
AD	0.0557			
CQ	135.2399			
UQI	1			
# 5				
IF	1			
SSIM	1			
RMSE	0			
PSNR	99			
AD	0			
CQ	135.051			
UQI	1			
# 6				
IF	0.9999			
SSIM	0.9834			
RMSE	0.9418			
PSNR	48.6513			
AD	0.0991			
CQ	1			
UQI	3.31E+05			
# 7				
IF	0.9999			
SSIM	0.9833			


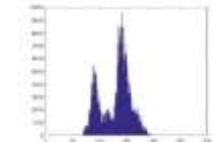

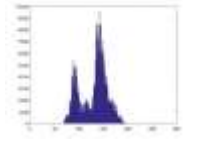

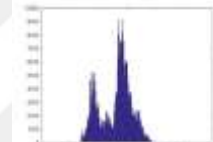

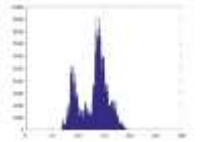

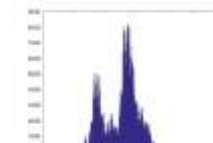



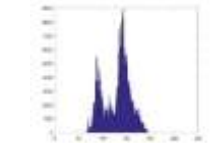

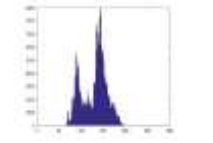
RMSE	0.9448			
PSNR	48.6238			
AD	0.1006			
CQ	135.186			
UQI	1			
# 8				
IF	1			
SSIM	0.9856			
RMSE	0.8114			
PSNR	49.9456			
AD	0.0839			
CQ	137.1369			
UQI	1			
# 9				
IF	1			
SSIM	0.9842			
RMSE	0.8495			
PSNR	49.5473			
AD	0.0897			
CQ	138.2878			
UQI	1			
# 10				
IF	1			
SSIM	0.9838			
RMSE	0.9123			
PSNR	48.9284			
AD	0.0977			
CQ	138.1625			
UQI	1			


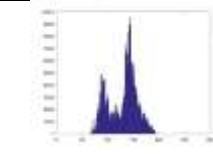

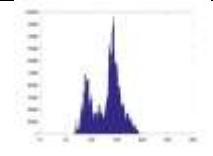

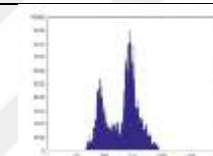

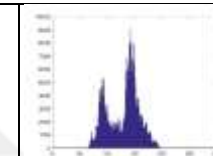

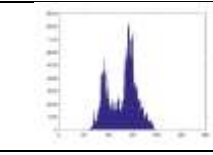

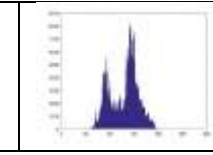

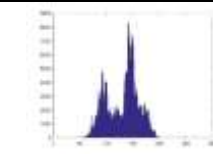

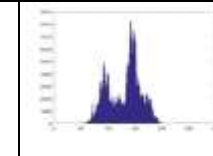
# 11				
IF	1.0000			
SSIM	0.9944			
RMSE	0.4727			
PSNR	54.6398			
AD	0.0426			
CQ	138.1989			
UQI	1.0000			
# 12				
IF	1.0000			
SSIM	0.9941			
RMSE	0.5172			
PSNR	53.8584			
AD	0.0451			
CQ	138.6082			
UQI	1.0000			
# 13				
IF	1.0000			
SSIM	0.9944			
RMSE	0.4456			
PSNR	55.1522			
AD	0.0369			
CQ	139.6286			
UQI	1.0000			
# 14				
IF	1.0000			
SSIM	0.9963			
RMSE	0.3189			
PSNR	58.0573			


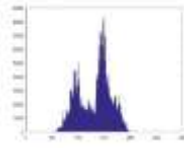

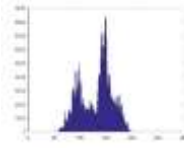

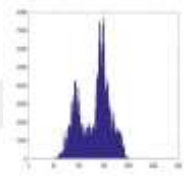

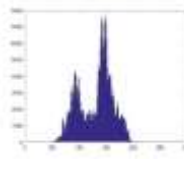

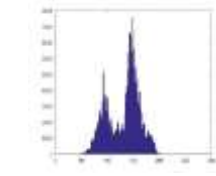

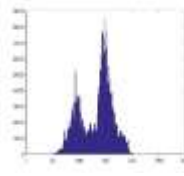
AD	0.0212			
CQ	140.3225			
UQI	1.0000			
# 15				
IF	1.0000			
SSIM	0.9953			
RMSE	0.3666			
PSNR	56.8463			
AD	0.0270			
CQ	141.2704			
UQI	1.0000			

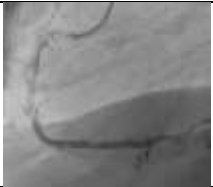
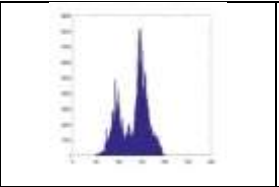

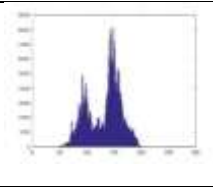

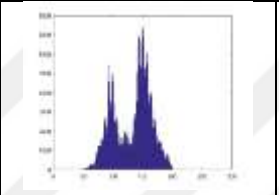

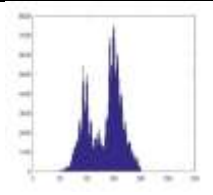

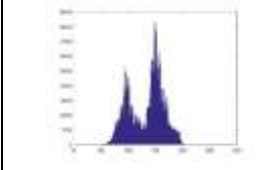

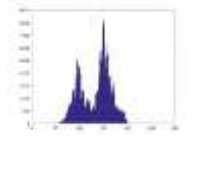

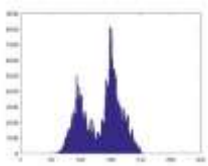
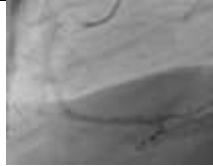
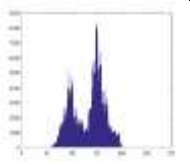
APPENDIX B

THE QUALITY MEASUREMENTS OF THE IMAGE (ANGINA PECTORIS) AFTER THE APPLICATION OF WAVELET (BIOR 2.2)

Video#	Original		Enhanced	
# 1				
IF	1			
SSIM	0.9978			
RMSE	0.2051			
PSNR	61.8913			
AD	0.0108			
CQ	135.21			
UQI	1			
# 2				
IF	1			
SSIM	0.9973			
RMSE	0.2177			
PSNR	61.3754			
AD	0.0116			
CQ	135.225			
UQI	1			
# 3				
IF	1			
SSIM	0.997			
RMSE	0.2421			
PSNR	60.4525			
AD	0.0152			
CQ	135.3869			
UQI	1			
# 4				

IF	1			
SSIM	0.9967			
RMSE	0.2754			
PSNR	59.3319			
AD	0.0181			
CQ	135.2146			
UQI	1			
# 5				
IF	1			
SSIM	0.996			
RMSE	0.3392			
PSNR	57.5214			
AD	0.0263			
CQ	135.0509			
UQI	1			
# 6				
IF	1			
SSIM	0.9938			
RMSE	0.4417			
PSNR	55.2276			
AD	0.0402			
CQ	135.0978			
UQI	1			
# 7				
IF	1			
SSIM	0.9937			
RMSE	0.415			
PSNR	59.132			
AD	0.039			
CQ	135.1694			
UQI	1			
# 8				

IF	1			
SSIM	0.9961			
RMSE	0.3203			
PSNR	58.021			
AD	0.0272			
CQ	137.1175			
UQI	1			
# 9				
IF	1			
SSIM	0.995			
RMSE	0.3834			
PSNR	56.4574			
AD	0.033			
CQ	138.2724			
UQI	1			
# 10				
IF	1			
SSIM	0.9941			
RMSE	0.426			
PSNR	55.5421			
AD	0.0378			
CQ	138.1476			
UQI	1			
# 11				
IF	1.0000			
SSIM	0.9931			
RMSE	0.4836			
PSNR	54.4409			
AD	0.0457			
CQ	138.1988			
UQI	1.0000			

# 12				
IF	1.0000			
SSIM	0.9934			
RMSE	0.4949			
PSNR	54.2403			
AD	0.0459			
CQ	138.6099			
UQI	1.0000			
# 13				
IF	1.0000			
SSIM	0.9941			
RMSE	0.3995			
PSNR	56.1013			
AD	0.0345			
CQ	139.6283			
UQI	1.0000			
# 14				
IF	1.0000			
SSIM	0.9951			
RMSE	0.3342			
PSNR	57.6496			
AD	0.0248			
CQ	140.3227			
UQI	1.0000			
# 15				
IF	0.9963			
SSIM	0.2045			
RMSE	8.3382			
PSNR	29.7094			
AD	3.0246			

CQ	140.1475
UQI	0.9960

